

RWA

**Open-Section Stiffened Composite Panel Coefficients
for Finite Element Analysis**

by

Mark Ronald Pickenheim

B.S. May 1992, Pennsylvania State University

A Thesis submitted to

The Faculty of

The School of Engineering and Applied Science
of The George Washington University in partial satisfaction
of the requirements for the degree of Master of Science

August 1994

Thesis directed by

Dr. Robert H. Tolson

Professor of Engineering and Applied Sciences

The George Washington University

This research was conducted at NASA LaRC

ABSTRACT

With the pursuit of technology for the High Speed Civil Transport (HSCT) and National Aerospace Plane (NASP), accurate preliminary structural analysis methods are necessary to arrive at the optimal design of the concept vehicle. Methods of capturing complicated 3-D thermoelastic behavior of stiffened composite panels with planar finite elements have become an important research area. Such an approach allows use of coarse finite element meshes to achieve accurate results for complete vehicle structural sizing and weight prediction from analysis of critical in-flight loads. A method for quantifying behavior of a hat-stiffened panel using smeared panel coefficients was developed for application to NASP research. This thesis examines honeycomb sandwich and blade-stiffened, T-stiffened, and orthogrid open-section panel concepts using the same method and compares behavior with detailed 3-D finite element reference models. Unique behavior specific to a particular stiffening concept must be determined to capture true panel behavior beyond the basic formulation of panel coefficients. For open-section stiffening geometry, it was found in general that the panel shear and twisting coefficients must be completed to capture full panel behavior. This work is intended to be applied to preliminary vehicle analysis of launch vehicles through implementation in a sizing code. The ability to formulate sandwich and open-section composite stiffened panels using the smeared panel coefficient method is achieved.

ACKNOWLEDGMENTS

I would like to thank everyone at the Vehicle Analysis Branch (VAB) for their help, guidance, and resources led by Chuck Eldred. God knows I'll never forget Garry Qualls and all those crazy stories he made up, plus all of the nutty times with Mark Johnson and Jason Bacon. For their technical assistance I would like to thank Jim Robinson and Chauncey Wu. For his unwavering guidance and just always seeming to know what the heck was going on and be totally relaxed and in control about it no matter what, I would like to thank Larry Rowell. In addition, this work wouldn't have been possible without the original work and continued guidance of Craig Collier who has been extremely helpful and insightful. I would like to also thank the members of my thesis committee including my advisor Dr. Robert Tolson, Dr. Myers, Dr. Raju, and Chauncey Wu. Final thanks to John Aguirre and his cats for putting up with me, and of course my whole family.

TABLE OF CONTENTS

ABSTRACT	i
ACKNOWLEDGMENTS	ii
TABLE OF CONTENTS	iii
LIST OF TABLES AND FIGURES	v
NOMENCLATURE	vi
1.0 INTRODUCTION	1
2.0 BACKGROUND AND MOTIVATION	2
2.1 Common approximate methods for stiffened panel analysis	2
2.2 Capturing unsymmetric and coupled panel behavior	3
2.3 Purpose and scope	5
3.0 ANALYSIS METHOD	7
3.1 Review of classical lamination theory	7
3.2 Panel elastic coefficient formulation	13
3.3 Panel thermal coefficient formulation	17
3.4 Behavior unique to a panel construction type	19
3.5 Post-processing of stiffened panels	20
4.0 DERIVATION OF PANEL COEFFICIENTS	22
4.1 Honeycomb sandwich panel	22
4.2 Blade-stiffened panel	24
4.3 T-stiffened panel	25
4.4 Orthogrid panel	27
4.5 Notes on derived panel coefficients	29
5.0 ANALYSIS AND DISCUSSION	31
5.1 Method of obtaining reference panel coefficients	31
5.2 Use of effective reduced laminate stiffness	32

5.3	Panel coefficient analysis	34
5.4	Additional stiffness for panels with unsupported stringers	36
5.5	Summary of derived panel coefficients	37
6.0	CONCLUDING REMARKS	41
7.0	REFERENCES	43

LIST OF TABLES AND FIGURES

Table 5.1: <i>Comparison of approximated laminate properties to classical lamination theory using $[0/+45/-45/90]_s$ lay-up with 8, 16, and 24 plies.</i>	33
Figure 2.1: <i>Two common approximate methods of stiffened panel analysis.</i>	3
Figure 2.2: <i>Geometry of a typical composite laminate and geometry of hat-stiffened composite panel.</i>	5
Figure 3.1: <i>Rotation of lamina axes.</i>	9
Figure 3.2: <i>Laminate configuration.</i>	10
Figure 3.3: <i>Stress resultant nomenclature in laminate coordinate system.</i>	11
Figure 3.4: <i>Geometry of hat-stiffened panel for panel coefficient formulation.</i>	16
Figure 4.1: <i>Honeycomb sandwich panel.</i>	22
Figure 4.2: <i>Blade-stiffened panel.</i>	24
Figure 4.3: <i>T-stiffened panel.</i>	26
Figure 4.4: <i>Orthogrid panel.</i>	28
Figure 5.1: <i>Open-section beam geometry for T-stiffened panel.</i>	37
Figure 5.2: <i>Boundary conditions and applied loads for stiffened panel examples.</i>	38
Figure 5.3: <i>Displacement in the out-of-plane direction (top) and percent difference of edge deflection (bottom) for blade-stiffened composite panel.</i>	39
Figure 5.4: <i>Displacement in the out-of-plane direction (top) and percent difference of edge deflection (bottom) for T-stiffened composite panel.</i>	40

NOMENCLATURE

LAMINA/PLY

E_1, E_2, G_{12}	Moduli of elasticity in 1-2 directions and in-plane shear modulus, respectively
ν_{12}, ν_{21}	Poisson ratios
α_1, α_2	Thermal expansion coefficients in the 1-2 directions
$\sigma_1, \sigma_2, \tau_{12}$	Ply stress in the 1-2 directions and in-plane shear stress
$\varepsilon_1, \varepsilon_2, \gamma_{12}$	Ply strain in the 1-2 directions and in-plane shear stress
θ	Angle between lamina 1-axis and the global X-axis
$\sigma_x, \sigma_y, \tau_{xy}$	Ply stress transformed to global axes
$\varepsilon_x, \varepsilon_y, \gamma_{xy}$	Ply strain transformed to global axes
Q_{ij}	Constitutive matrix of a unidirectional ply relating stress to strain (3x3)
\bar{Q}_{ij}	Constitutive matrix of a ply of general orientation transformed to global coordinates (3x3)
Φ_i	Thermal constitutive vector of a unidirectional ply (3x1)
$\bar{\Phi}_i$	Thermal constitutive vector transformed to global coordinates (3x1)

LAMINATE

A_{ij}	Membrane expansion stiffness matrix (3x3)
B_{ij}	Membrane-bending coupling matrix (3x3)
D_{ij}	Bending stiffness matrix (3x3)
A_i^α	Membrane thermal coefficients (3x1)
B_i^α	Membrane-bending thermal coefficients (3x1)
D_i^α	Thermal bending coefficients (3x1)
\bar{Q}_{ij}^*	Laminate effective reduced elastic stiffness (3x3)
$\bar{\Phi}_i^*$	Laminate effective reduced thermal stiffness (3x1)
t	Laminate thickness

PANEL

<i>longitudinal</i>	In-plane direction along panel stringers
<i>transverse</i>	In-plane direction perpendicular to panel stringers
A_{ij}^p	Membrane expansion stiffness matrix (3x3)
B_{ij}^p	Membrane-Bending coupling matrix (3x3)
D_{ij}^p	Bending stiffness matrix (3x3)
$A_i^{p\alpha}$	Membrane thermal expansion stiffness vector (3x1)
$B_i^{p\alpha}$	Membrane-bending thermal coupling stiffness vector (3x1)
$D_i^{p\alpha}$	Bending thermal stiffness vector (3x1)
$\alpha_{A_i}^p$	Membrane thermal coefficients (3x1)
$\alpha_{B_i}^p$	Membrane-bending thermal coefficients (3x1)
$\alpha_{D_i}^p$	Bending thermal coefficients (3x1)
ΔT	In-plane temperature gradient (scalar)
ΔG	Through-the-thickness temperature gradient (scalar)

1.0 INTRODUCTION

Fiber reinforced composite materials are often used in the multidisciplinary process of aerospace vehicle conceptual structural design. With a large number of design variables in ply stacking sequences and orientations, advanced composite materials offer weight and strength advantages. The need for quick preliminary analysis and the complexities of composite materials often lead to analytic approximations during structural analysis. Due to simplifications, common symmetric property methods of stiffened panel analysis produce significant error in predicting panel forces and moments. Use of these methods can lead conceptual analysts to arrive at a non-optimum design [1].

Hot-environment analyses, where in-plane and through-the-thickness thermal gradients are encountered, are necessary for accurate load prediction of concept vehicles. Other application areas such as cryogenic fuel tank design require similar analyses. The formulation of the thermal behavior of composite materials is complex and often ignored. A method outlined by Collier [2] may be the first formulation to define through-the-thickness thermal gradient behavior for composite panel analysis.

This work extends the method presented by Collier in which equivalent smeared plate properties of stiffened composite panels are formulated. Panel elastic coefficients are in the form of A , B , and D constitutive matrices common to composite laminate analysis. Panel thermal expansion vectors are formulated for hot-environment applications. Using a coarse mesh of shell finite elements based on this method, accurate preliminary structural analysis can be performed for an entire vehicle [2]. Post-processing to determine panel failure and stability is easily performed using finite element stress resultants.

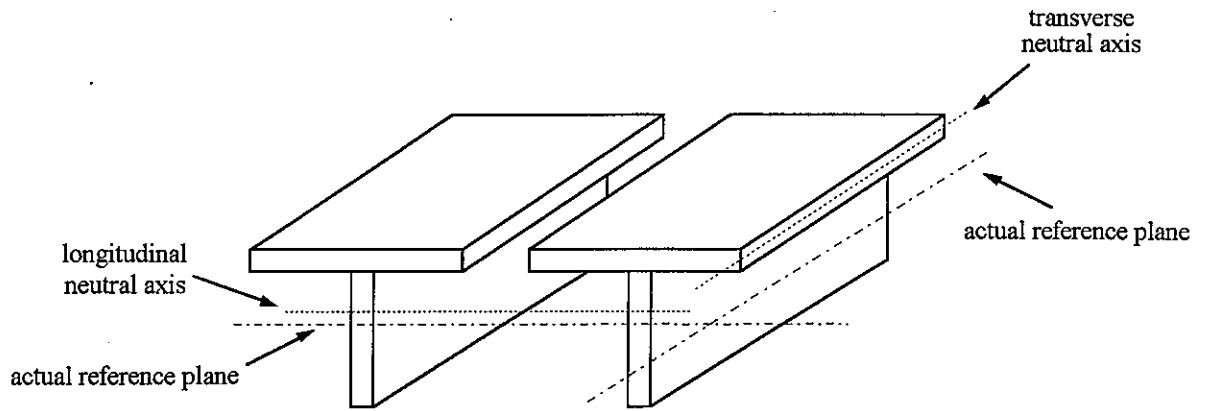
2.0 BACKGROUND AND MOTIVATION

It is necessary first to review common approximate methods of analyzing stiffened panels and the shortcomings of these analyses. The advantage of being able to fully capture the unsymmetric and coupled behavior of composite stiffened panels with a panel coefficient method is discussed. The goals and scope for the work to be performed are then defined followed by an outline of this thesis.

2.1 Common approximate methods for stiffened panel analysis

Two methods of approximating stiffened panel behavior are the detached wide beam and symmetric panel analogies which are shown in Figure 2.1. The first method considers the panel as a series of detached beams forming the stiffened geometry of the panel. The longitudinal direction refers to the panel in-plane stiffened direction and the transverse direction refers to the in-plane direction perpendicular to the stiffeners. Using the parallel axis theorem, membrane and bending stiffness properties are calculated about the individual panel longitudinal and transverse neutral axes. However, these properties are obtained using an inconsistent reference plane which has the effect of omitting the unsymmetric membrane-bending coupled behavior of the panel. Further, because the panel has been broken into pieces, coupling of behavior in the in-plane longitudinal and transverse directions is ignored [4].

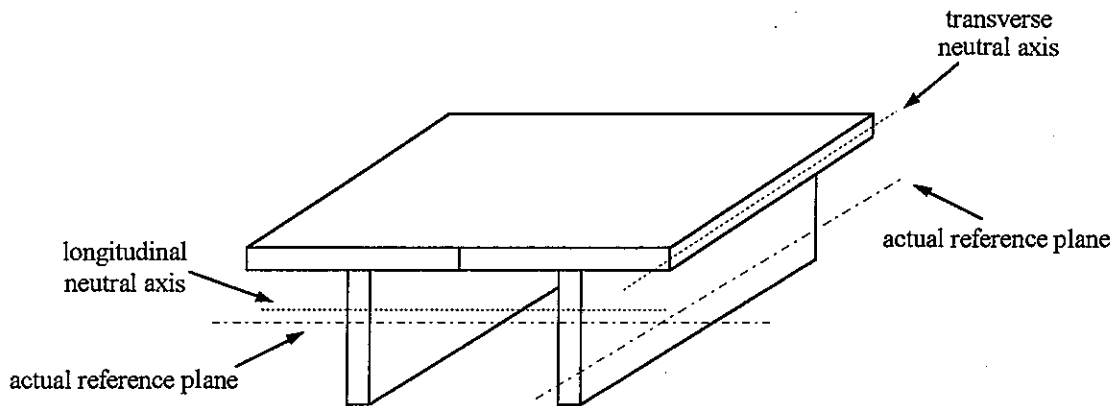
The symmetric panel method uses plate formulation which includes in-plane longitudinal and transverse coupled behavior. Membrane and bending properties are calculated in the same manner as the detached beam method omitting unsymmetric membrane-bending coupling. Reference [1] shows that significant errors can result in symmetric panel analysis when compared to an analysis utilizing the full unsymmetric and coupled properties inherent in stiffened panels.



Detached Wide Beam Method

missing:

- In-plane longitudinal and transverse coupling
- Unsymmetric membrane-bending coupling



Symmetric Panel Method

missing:

- Unsymmetric membrane-bending coupling

Figure 2.1: *Two common approximate methods of stiffened panel analysis.*

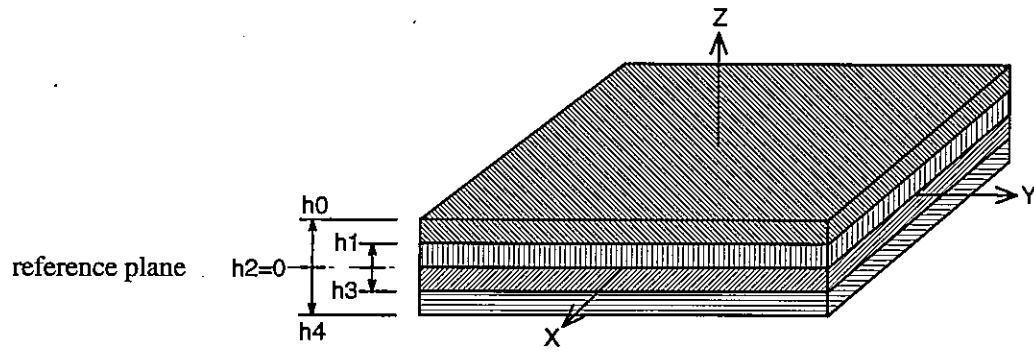
2.2 Capturing unsymmetric and coupled panel behavior

The geometry of a typical composite laminate is illustrated in Figure 2.2A. By considering the individual ply material properties and the respective distances h_i from a common reference plane, membrane and bending properties of the composite laminate can be defined with classical lamination theory. By extending this method of property

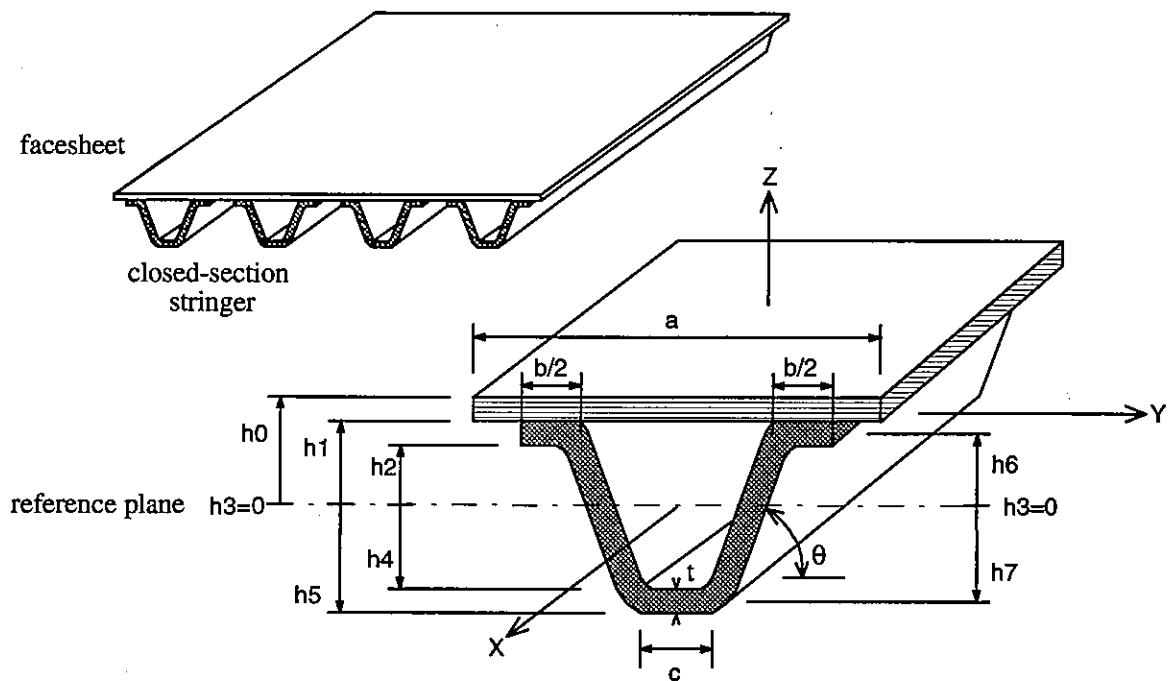
formulation to the hat-stiffened cross-section illustrated in Figure 2.2B, an accurate representation of the elastic behavior of a composite stiffened panel can be defined in an average sense. Unsymmetric membrane-bending coupling is captured by use of a consistent reference plane. Longitudinal and transverse panel properties are coupled by use of plate formulation.

The smeared property panel coefficients are equivalent A , B , and D elastic membrane and bending constitutive relations common to the analysis of composite laminates. Use of these coefficients models behavior as a stiffened composite panel instead of a general laminate. Panel thermal characteristics are described in formulated thermal expansion coefficient vectors $\{\alpha_A\}$, $\{\alpha_B\}$, $\{\alpha_D\}$. The thermoelastic coefficients are used to supply properties for planar meshes of shell elements to a general purpose finite element program such as NASTRAN. Loads, temperatures, and boundary conditions are defined in the analysis. Using the stress resultants obtained from the finite element solution, strain is calculated at desired stations in the panel for appropriate failure and stability analyses. This method of stiffened panel analysis can be integrated into a panel sizing code for structural weight estimates of aerospace vehicles.

Depending on the panel stringer geometry, additional effects must be identified that are not considered in the basic formulation of panel coefficients. For closed-section stringers, additional in-plane transverse bending stiffness results from longitudinal panel stiffening. In addition, for both open-section and closed-section stringers, significant additional panel shear and twisting stiffness results. By considering how the panel is attached in service, the additional effects of the stringers not included in the basic formulation of panel coefficients can be obtained. Different panel behavior is found depending on how the panel stringers are supported. In general, stringer ends are built-in to supporting frames, are tapered into the facesheet at supporting frames, or are free with no support between frames.



A. Geometry of typical composite laminate



B. Geometry of hat-stiffened panel

Figure 2.2: *Geometry of a typical composite laminate and geometry of hat-stiffened composite panel.*

2.3 Purpose and scope

In this work, coefficients are formulated for stiffened panels with open-section stringers as was accomplished for the closed-section hat-stiffened panel presented in

reference [4]. For the hat panel shown in Figure 2.2, the stiffener construction provided significant additional stiffness that had to be quantified to accurately determine panel coefficients. It is necessary to compare formulated coefficients to reference coefficients obtained from finite element models to determine behavior unique to a particular panel stiffening configuration.

Reference panel coefficients are obtained by applying unit strains and curvatures to detailed 3-D shell finite element models. Behavior unique to a panel geometry must be identified to complete the panel coefficients. In the basic procedure, the shear and twisting stiffness of the panel is obtained from the facesheet. Since additional shear and twisting stiffness provided by the stringers is not included, the effects of the stringers must be examined. It is also necessary to examine in-plane transverse coefficients since these are significantly affected for closed-section geometry and are not addressed in the basic formulation of panel coefficients [4].

Chapter 3 reviews classical lamination theory for composite laminates and discusses the basic method of panel coefficient formulation as outlined in reference [2]. Panel coefficients for honeycomb sandwich, blade-stiffened, T-stiffened, and orthogrid (having stringers in both the longitudinal and transverse directions) panels are derived in Chapter 4. In Chapter 5, comparison is made to reference panel coefficients obtained from 3-D finite element modeling and additional terms necessary to fully characterize the basic panel coefficients is explored.

3.0 ANALYSIS METHOD

The basic method of formulating composite stiffened panel coefficients is presented in Section 3.2. Since a knowledge of classical lamination theory is essential to fully understand the approach, it is outlined first.

3.1 Review of classical lamination theory

Composite laminates consist of plies of fibers oriented in a matrix and stacked in such a way as to increase the laminate structural efficiency. Recent technological developments include high modulus fibers in organic, ceramic, and metallic matrices [5].

In general each layer in classical lamination theory is considered to be orthotropic (having three planes of symmetry) and is referred to as a lamina. Using $\sigma_1, \sigma_2, \tau_{12}$ and $\varepsilon_1, \varepsilon_2, \gamma_{12}$ in place of the tensor notation $\sigma_{ij}, \varepsilon_{ij}$, an orthotropic lamina in a state of plane stress is characterized by the following constitutive relationship:

$$\begin{Bmatrix} \sigma_1 \\ \sigma_2 \\ \tau_{12} \end{Bmatrix} = \begin{bmatrix} Q_{11} & Q_{12} & 0 \\ Q_{12} & Q_{22} & 0 \\ 0 & 0 & Q_{33} \end{bmatrix} \begin{Bmatrix} \varepsilon_1 \\ \varepsilon_2 \\ \gamma_{12} \end{Bmatrix} \quad (3.1)$$

where the 1-2-3 coordinate system is referred to as the principal or material coordinate directions. The fiber is oriented along the 1 direction, the 2 direction is transverse to the fibers in-plane, and the 3 direction is transverse to the fibers out-of-plane. The Q_{ij} terms in Equation 3.1 are given by

$$\begin{aligned}
Q_{11} &= \frac{E_{11}}{1 - \nu_{12}\nu_{21}} \\
Q_{22} &= \frac{E_{22}}{1 - \nu_{12}\nu_{21}} \\
Q_{12} &= \frac{\nu_{21}E_{11}}{1 - \nu_{12}\nu_{21}} = \frac{\nu_{12}E_{22}}{1 - \nu_{12}\nu_{21}} \\
Q_{33} &= G_{12}
\end{aligned} \tag{3.2}$$

where E_{11} , E_{22} , G_{12} , and ν_{12} are the 4 independent engineering quantities of the orthotropic lamina. E_{11} is Young's modulus along the fibers, E_{22} is Young's modulus transverse to the fibers, ν_{12} is Poisson's ratio as measured from the transverse contraction under uniaxial tension parallel to the fibers, G_{12} is the shear modulus relative to the 1-2 plane, and $\nu_{21} = (E_{22} / E_{11})\nu_{12}$.

As shown in Figure 3.1, Equation 3.1 may be transformed into an arbitrary global coordinate system oriented at an angle θ relative to the material axes

$$\begin{Bmatrix} \sigma_x \\ \sigma_y \\ \tau_{xy} \end{Bmatrix} = \begin{bmatrix} \bar{Q}_{11} & \bar{Q}_{12} & \bar{Q}_{13} \\ \bar{Q}_{12} & \bar{Q}_{22} & \bar{Q}_{23} \\ \bar{Q}_{13} & \bar{Q}_{23} & \bar{Q}_{33} \end{bmatrix} \begin{Bmatrix} \epsilon_x \\ \epsilon_y \\ \gamma_{xy} \end{Bmatrix} \tag{3.3}$$

The transformed lamina constitutive matrix terms are given by the tensor relationships:

$$\begin{aligned}
\bar{Q}_{11} &= Q_{11} \cos^4 \theta + 2(Q_{12} + 2Q_{33}) \sin^2 \theta \cos^2 \theta + Q_{22} \sin^4 \theta \\
\bar{Q}_{12} &= (Q_{11} + Q_{22} - 4Q_{33}) \sin^2 \theta \cos^2 \theta + Q_{12} (\sin^4 \theta \cos^4 \theta) \\
\bar{Q}_{22} &= Q_{22} \cos^4 \theta + 2(Q_{12} + 2Q_{33}) \sin^2 \theta \cos^2 \theta + Q_{11} \sin^4 \theta \\
\bar{Q}_{13} &= (Q_{11} - Q_{12} - 2Q_{33}) \sin \theta \cos^3 \theta + (Q_{12} - Q_{22} + 2Q_{33}) \sin^3 \theta \cos \theta \\
\bar{Q}_{23} &= (Q_{11} - Q_{12} - 2Q_{33}) \sin^3 \theta \cos \theta + (Q_{12} - Q_{22} + 2Q_{33}) \sin \theta \cos^3 \theta \\
\bar{Q}_{33} &= (Q_{11} + Q_{22} - 2Q_{12} - 2Q_{33}) \sin^2 \theta \cos^2 \theta + Q_{33} (\sin^4 \theta + \cos^4 \theta)
\end{aligned} \tag{3.4}$$

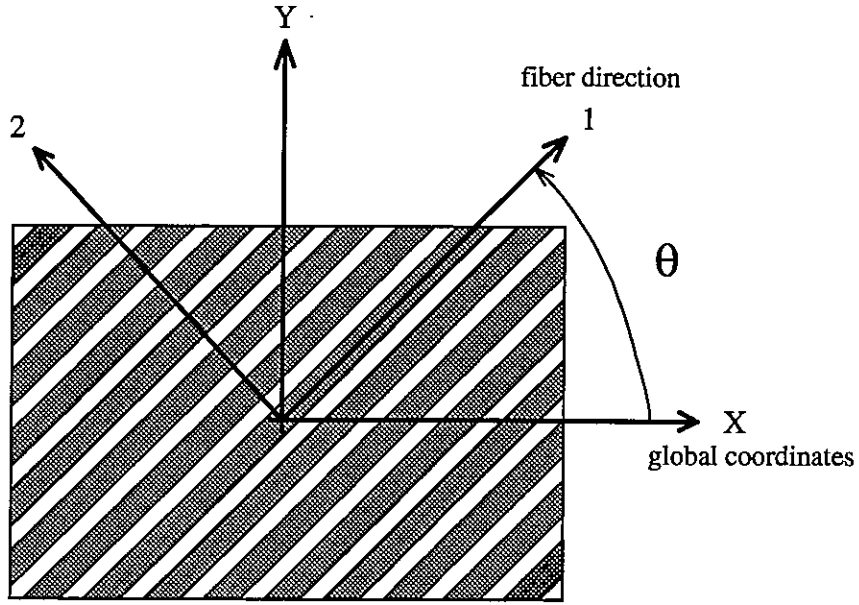


Figure 3.1: *Rotation of lamina axes.*

Shown in Figure 3.2, individual plies are stacked bottom to top in a desired stacking sequence to form a laminate. For example, the notation $[0/+45/-45/90]_s$ represents a symmetric stack of 8 plies oriented $[0/+45/-45/90/90/-45/+45/0]$ degrees with respect to the laminate coordinate system. The laminate behavior for applied loads can be described using the Kirchoff assumption that plane sections remain plane after deformation, which can be written

$$\begin{Bmatrix} \epsilon_x \\ \epsilon_y \\ \gamma_{xy} \end{Bmatrix} = \begin{Bmatrix} \epsilon_x^o \\ \epsilon_y^o \\ \gamma_{xy}^o \end{Bmatrix} + z \begin{Bmatrix} \kappa_x \\ \kappa_y \\ \kappa_{xy} \end{Bmatrix} \quad (3.5)$$

where ϵ_i^o are the reference plane strains, κ_i are the reference plane curvatures, and z is the distance from the reference plane. The stress in the k^{th} layer of the laminate can be computed then as

$$\{\sigma\}_k = [\bar{Q}]_k \{\epsilon^o\} + z_k [\bar{Q}]_k \{\kappa\} \quad (3.6)$$

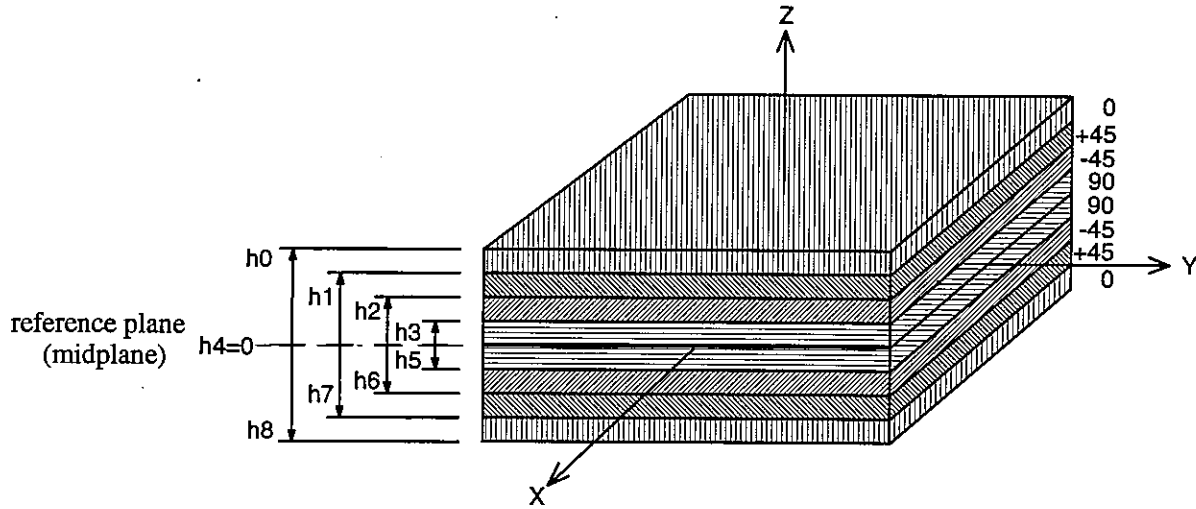


Figure 3.2: Laminate configuration.

Strain is therefore linear through the thickness of the laminate (as a consequence of the assumption that plane sections remain plane) and stresses vary discontinuously between lamina. Stress resultants can be written in the form

$$\begin{Bmatrix} N_x \\ N_y \\ N_{xy} \end{Bmatrix} = \int_{-t/2}^{+t/2} \begin{Bmatrix} \sigma_x \\ \sigma_y \\ \tau_{xy} \end{Bmatrix} dz \quad (3.7)$$

The stress resultants shown in Figure 3.3 are the stresses of the laminate integrated through-the-thickness and have units of force or moment per unit length. The integral in Equation 3.7 can be written as the sum of n integrals over each layer of the laminate:

$$\begin{Bmatrix} N_x \\ N_y \\ N_{xy} \end{Bmatrix} = \sum_{k=1}^n \int_{h_{k-1}}^{h_k} \begin{Bmatrix} \sigma_x \\ \sigma_y \\ \tau_{xy} \end{Bmatrix} dz \quad (3.8)$$

After substitution of Equation 3.6, Equation 3.8 becomes

$$\begin{Bmatrix} N_x \\ N_y \\ N_{xy} \end{Bmatrix} = \sum_{k=1}^n \left\{ \begin{bmatrix} \bar{Q}_{11} & \bar{Q}_{12} & \bar{Q}_{13} \\ \bar{Q}_{12} & \bar{Q}_{22} & \bar{Q}_{23} \\ \bar{Q}_{13} & \bar{Q}_{23} & \bar{Q}_{33} \end{bmatrix}_k \begin{Bmatrix} \epsilon_x^o \\ \epsilon_y^o \\ \gamma_{xy}^o \end{Bmatrix}_{h_{k-1}}^{h_k} + \begin{bmatrix} \bar{Q}_{11} & \bar{Q}_{12} & \bar{Q}_{13} \\ \bar{Q}_{12} & \bar{Q}_{22} & \bar{Q}_{23} \\ \bar{Q}_{13} & \bar{Q}_{23} & \bar{Q}_{33} \end{bmatrix}_k \begin{Bmatrix} \kappa_x \\ \kappa_y \\ \kappa_{xy} \end{Bmatrix}_{h_{k-1}}^{h_k} \int_{h_{k-1}}^{h_k} z dz \right\} \quad (3.9)$$

Equation 3.9 is then written in the form

$$\begin{Bmatrix} N_x \\ N_y \\ N_{xy} \end{Bmatrix} = \begin{bmatrix} A_{11} & A_{12} & A_{13} \\ A_{12} & A_{22} & A_{23} \\ A_{13} & A_{23} & A_{33} \end{bmatrix}_k \begin{Bmatrix} \epsilon_x^o \\ \epsilon_y^o \\ \gamma_{xy}^o \end{Bmatrix} + \begin{bmatrix} B_{11} & B_{12} & B_{13} \\ B_{21} & B_{22} & B_{23} \\ B_{31} & B_{32} & B_{33} \end{bmatrix}_k \begin{Bmatrix} \kappa_x \\ \kappa_y \\ \kappa_{xy} \end{Bmatrix} \quad (3.10)$$

where

$$A_{ij} = \sum_{k=1}^n (\bar{Q}_{ij})_k (h_k - h_{k-1})$$

$$2B_{ij} = \sum_{k=1}^n (\bar{Q}_{ij})_k (h_k^2 - h_{k-1}^2)$$

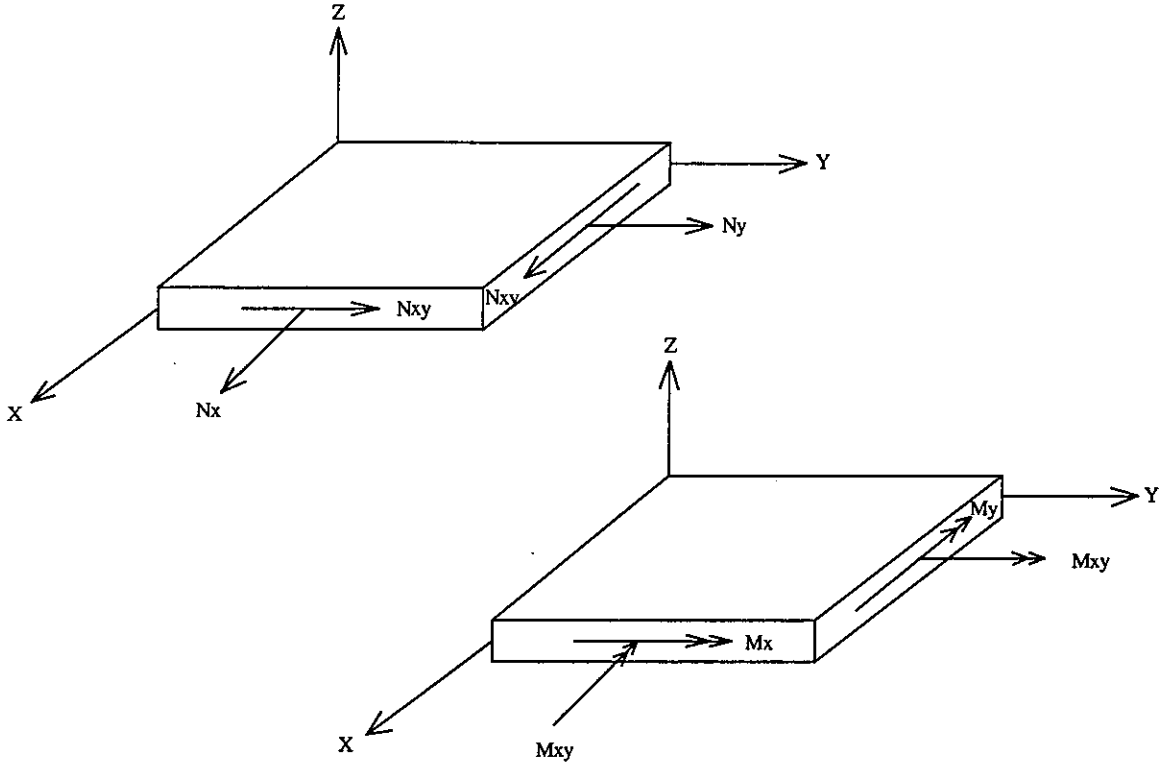


Figure 3.3: Stress resultant nomenclature in laminate coordinate system.

In Equation 3.10, the A_{ij} terms describe behavior between reference plane strains and reference plane stress resultants. The B_{ij} terms describe coupling behavior between reference plane curvatures and reference plane stress resultants. Similarly, the moment resultants are given by

$$\begin{Bmatrix} M_x \\ M_y \\ M_{xy} \end{Bmatrix} = \int_{-t/2}^{+t/2} \begin{Bmatrix} \sigma_x \\ \sigma_y \\ \tau_{xy} \end{Bmatrix} z dz \quad (3.11)$$

which, after substitution of Equation 3.6 and integration, yields

$$\begin{Bmatrix} M_x \\ M_y \\ M_{xy} \end{Bmatrix} = \begin{bmatrix} B_{11} & B_{12} & B_{13} \\ B_{21} & B_{22} & B_{23} \\ B_{31} & B_{32} & B_{33} \end{bmatrix}_k \begin{Bmatrix} \varepsilon_x^o \\ \varepsilon_y^o \\ \gamma_{xy}^o \end{Bmatrix} + \begin{bmatrix} D_{11} & D_{12} & D_{13} \\ D_{12} & D_{22} & D_{23} \\ D_{13} & D_{23} & D_{33} \end{bmatrix}_k \begin{Bmatrix} \kappa_x \\ \kappa_y \\ \kappa_{xy} \end{Bmatrix} \quad (3.12)$$

where

$$2B_{ij} = \sum_{k=1}^n (\bar{Q}_{ij})_k (h_k^2 - h_{k-1}^2)$$

$$3D_{ij} = \sum_{k=1}^n (\bar{Q}_{ij})_k (h_k^3 - h_{k-1}^3)$$

In Equation 3.12, the B_{ij} terms describe coupling behavior between reference plane strains and reference plane moment resultants and are the same as previously derived. The D_{ij} terms describe behavior between reference plane curvatures and reference plane moment resultants. Combining these results leads to the following constitutive relationship for small normal curvatures of a composite laminate:

$$\begin{Bmatrix} N_i \\ M_i \end{Bmatrix} = \begin{bmatrix} A_{ij} & B_{ij} \\ B_{ij} & D_{ij} \end{bmatrix} \begin{Bmatrix} \varepsilon_j^o \\ \kappa_j \end{Bmatrix} \quad (3.13)$$

The 3x3 matrices A , B , and D in Equation 3.13 describe laminate behavior. These coefficients can be entered into a finite element code for laminate analysis of shell

finite elements. Structural analysis of the stiffened panel will return reference-plane strains and curvatures which can be used to determine strain through the thickness of the laminate for ply failure analysis. Often the midplane of the laminate is used as the reference plane. If the midplane is used as a reference plane and the ply lay-up is symmetric, the B_{ij} membrane-bending coupling terms vanish.

3.2 Panel elastic coefficient formulation

Reference [2] extends classical formulation of composite laminates to the cross-section of a composite stiffened panel. If the analogy is made that the laminates forming the stiffened panel are considered the plies of classical lamination theory, smeared panel coefficients $A_{ij}^p, B_{ij}^p, D_{ij}^p$ are obtained. This formulation allows 2-D shell elements to capture the elastic properties of complicated 3-D stiffened panels.

The limitations of this method are the same as those of classical lamination theory. The primary assumption of classical lamination theory is that plane sections remain plane and normal to the reference plane after deformation. To simplify the formulation of panel coefficients, it is assumed that only the laminate membrane extension terms A_{ij} are required to utilize composite material properties. This assumption, which eliminates the need to include cumbersome ply data, uses effective isotropic properties for the laminates comprising the panel. A constitutive matrix similar to that of a ply is obtained given by:

$$\bar{Q}_{ij}^* = \frac{A_{ij}}{t} \quad (3.14)$$

where t is the thickness of the laminate. Equation 3.14 defines averaged composite laminate properties in the stiffened panel in place of Equation 3.3 which defines ply properties in composite laminates. Panel coefficients are formulated as if each laminate of the panel construction is a ply with material properties defined by Equation 3.14.

Proceeding as illustrated in Figure 3.4, where each layer in the stiffened panel is a lamina with a constitutive matrix of \bar{Q}_{ij}^* , panel coefficients $A_{ij}^p, B_{ij}^p, D_{ij}^p$ are formulated. However, for the stiffening layer attached to the facesheet, only stiffness in the direction of reinforcement is considered. To correctly formulate the contribution to the panel coefficients, the stringer terms are multiplied by the ratio of the stiffener thickness parallel to the facesheet in the panel cross-section to the spacing between stringers. However these layers are not acting as plates and their \bar{Q}_{ij}^* must not include plate formulation. In general, for the stringer laminates \bar{Q}_{11}^* is instead the effective Young's modulus of the laminate

$$E_x = \frac{1}{A_{11}^{-1}t} \quad (3.15)$$

where A_{11}^{-1} is the coefficient from the inverted \mathbf{A} matrix of the stringer laminate and t is the laminate thickness.

Coefficients for the closed-section hat panel formulation follow. All distances included are signed distances from the reference plane in the panel out-of-plane direction. First the facesheet contributes to the panel coefficients. Referring to Figure 3.4, for $i, j=1,2,3$ the facesheet supplies:

$$\begin{aligned} A_{ij}^{hat} &= (\bar{Q}_{ij}^*)_{facesheet} (h_0 - h_1) \\ 2B_{ij}^{hat} &= (\bar{Q}_{ij}^*)_{facesheet} (h_0^2 - h_1^2) \\ 3D_{ij}^{hat} &= (\bar{Q}_{ij}^*)_{facesheet} (h_0^3 - h_1^3) \end{aligned} \quad (3.16)$$

The longitudinal coefficients of the panel are reinforced by the hat stiffeners. Assuming the same laminate is used for each section of the stringer, longitudinal panel coefficients are augmented from the following as the contribution of the top flange of the stringer:

$$\begin{aligned}
A_{11}^{hat} &: \left(\frac{b}{a}\right)(\overline{Q}_{ij}^*)_{stringer} (h_1 - h_2) \\
2B_{11}^{hat} &: \left(\frac{b}{a}\right)(\overline{Q}_{ij}^*)_{stringer} (h_1^2 - h_2^2) \\
3D_{11}^{hat} &: \left(\frac{b}{a}\right)(\overline{Q}_{ij}^*)_{stringer} (h_1^3 - h_2^3)
\end{aligned} \tag{3.17}$$

The ratio $\frac{b}{a}$ determines the average effect of the top flange on the smeared panel coefficients where a is the spacing between stringers.

The stringer web contributes the following to the panel coefficients:

$$\begin{aligned}
A_{11}^{hat} &: \left(\frac{2t}{a \sin \theta}\right)(\overline{Q}_{ij}^*)_{stringer} (h_6 - h_7) \\
2B_{11}^{hat} &: \left(\frac{2t}{a \sin \theta}\right)(\overline{Q}_{ij}^*)_{stringer} (h_6^2 - h_7^2) \\
3D_{11}^{hat} &: \left(\frac{2t}{a \sin \theta}\right)(\overline{Q}_{ij}^*)_{stringer} (h_6^3 - h_7^3)
\end{aligned} \tag{3.18}$$

The $\frac{2t}{\sin \theta}$ term is the thickness of the stringer web parallel to the facesheet in one stringer spacing. This thickness divided by panel stringer spacing a determines the average contribution of the web on the smeared panel coefficients.

Finally, the stringer bottom flange contributions to the panel coefficients are:

$$\begin{aligned}
A_{11}^{hat} &: \left(\frac{c}{a}\right)(\overline{Q}_{ij}^*)_{stringer} (h_4 - h_5) \\
2B_{11}^{hat} &: \left(\frac{c}{a}\right)(\overline{Q}_{ij}^*)_{stringer} (h_4^2 - h_5^2) \\
3D_{11}^{hat} &: \left(\frac{c}{a}\right)(\overline{Q}_{ij}^*)_{stringer} (h_4^3 - h_5^3)
\end{aligned} \tag{3.19}$$

The ratio $\frac{c}{a}$ determines the average effect of the bottom flange on the smeared panel coefficients.

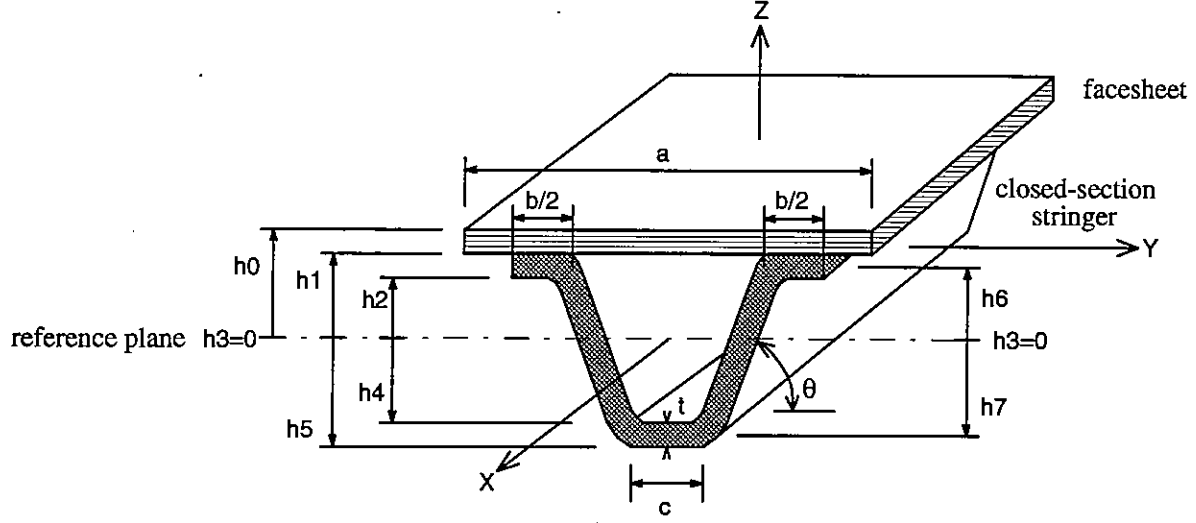


Figure 3.4: Geometry of hat-stiffened panel for panel coefficient formulation.

The basic formulation of coefficients for the hat-stiffened panel shown in Figure 3.4 is summarized as:

$$\begin{aligned}
 A_{ij}^{hat} &= (\bar{Q}_{ij}^*)_{facesheet} (h_0 - h_1) \\
 2B_{ij}^{hat} &= (\bar{Q}_{ij}^*)_{facesheet} (h_0^2 - h_1^2) \\
 3D_{ij}^{hat} &= (\bar{Q}_{ij}^*)_{facesheet} (h_0^3 - h_1^3)
 \end{aligned} \tag{3.20}$$

where the longitudinal coefficients are reinforced by the hats and are augmented by

$$\begin{aligned}
 A_{11}^{hat} &: \left(\frac{b}{a}\right)(\bar{Q}_{11}^*)_{stringer} (h_1 - h_2) + \left(\frac{2t}{a \sin \theta}\right)(\bar{Q}_{11}^*)_{stringer} (h_6 - h_7) + \left(\frac{c}{a}\right)(\bar{Q}_{11}^*)_{stringer} (h_4 - h_5) \\
 2B_{11}^{hat} &: \left(\frac{b}{a}\right)(\bar{Q}_{11}^*)_{stringer} (h_1^2 - h_2^2) + \left(\frac{2t}{a \sin \theta}\right)(\bar{Q}_{11}^*)_{stringer} (h_6^2 - h_7^2) + \left(\frac{c}{a}\right)(\bar{Q}_{11}^*)_{stringer} (h_4^2 - h_5^2) \\
 3D_{11}^{hat} &: \left(\frac{b}{a}\right)(\bar{Q}_{11}^*)_{stringer} (h_1^3 - h_2^3) + \left(\frac{2t}{a \sin \theta}\right)(\bar{Q}_{11}^*)_{stringer} (h_6^3 - h_7^3) + \left(\frac{c}{a}\right)(\bar{Q}_{11}^*)_{stringer} (h_4^3 - h_5^3)
 \end{aligned}$$

Contributions of the longitudinal stringer to any of the panel in-plane transverse or shear coefficients are not considered in the basic formulation. Complete panel

coefficients for the hat panel is given in reference [4] and consists of additional transverse panel bending stiffness and large amounts of additional panel shear and twisting stiffness from the "torque tubes" formed by the closed-section stringers. The method presented in this section is applied in the next chapter to the panel types considered in this thesis.

3.3 Panel thermal coefficient formulation

Two different types of thermal gradients can be applied to a panel. The in-plane temperature gradient is a temperature variation over the surface of the panel. A through-the-thickness gradient is the variation of temperature through the depth of the panel which is important for analysis of vehicles such as the NASP which cruise at high Mach numbers. The following thermal formulation of stiffened panel behavior is obtained directly from reference [2].

Thermal stiffness Φ_i is formulated as

$$\begin{Bmatrix} \Phi_1 \\ \Phi_2 \\ \Phi_3 \end{Bmatrix} = \begin{bmatrix} Q_{11} & Q_{12} & 0 \\ Q_{21} & Q_{22} & 0 \\ 0 & 0 & Q_{33} \end{bmatrix} \begin{Bmatrix} \alpha_1 \\ \alpha_2 \\ \alpha_3 \end{Bmatrix} \quad (3.21)$$

where α_1 is the coefficient of thermal expansion of the lamina in the fiber direction and α_2, α_3 are the coefficients of thermal expansion in the transverse and out-of-plane directions respectively. A second order tensor transformation is required to transform the thermal stiffness terms from lamina to laminate axes:

$$\begin{Bmatrix} \bar{\Phi}_1 \\ \bar{\Phi}_2 \\ \bar{\Phi}_3 \end{Bmatrix} = \begin{bmatrix} \cos^2 \theta & \sin^2 \theta & 2\cos\theta\sin\theta \\ \sin^2 \theta & \cos^2 \theta & -2\cos\theta\sin\theta \\ -\cos\theta\sin\theta & \cos\theta\sin\theta & \cos^2 \theta - \sin^2 \theta \end{bmatrix} \begin{Bmatrix} \Phi_1 \\ \Phi_2 \\ \Phi_3 \end{Bmatrix} \quad (3.22)$$

The term $\Phi_3 = 0$ because it is assumed $\alpha_3 = 0$. Thermal stiffness terms $\bar{\Phi}_i$ in Equation 3.22 reduce to

$$\begin{aligned}
\bar{\Phi}_1 &= \Phi_1 \cos^2 \theta + \Phi_2 \sin^2 \theta \\
\bar{\Phi}_2 &= \Phi_1 \sin^2 \theta + \Phi_2 \cos^2 \theta \\
\bar{\Phi}_3 &= (\Phi_2 - \Phi_1) \cos \theta \sin \theta
\end{aligned} \tag{3.23}$$

Classical lamination theory is used to determine laminate thermal vectors $A_i^\alpha, B_i^\alpha, D_i^\alpha$:

$$\begin{aligned}
A_i^\alpha &= \sum_{k=1}^n (\bar{\Phi}_i)_k (h_k - h_{k+1}) \\
2B_i^\alpha &= \sum_{k=1}^n (\bar{\Phi}_i)_k (h_k^2 - h_{k+1}^2) \\
3D_i^\alpha &= \sum_{k=1}^n (\bar{\Phi}_i)_k (h_k^3 - h_{k+1}^3)
\end{aligned} \tag{3.24}$$

As with the formulation of panel elastic stiffness, it is assumed that only A_i^α are needed to formulate panel thermal stiffness. The effective reduced laminate thermal stiffness is defined as

$$\bar{\Phi}_i^* = \frac{A_i^\alpha}{t} \tag{3.25}$$

where t is the laminate thickness.

Panel thermal stiffness vectors $A_i^{p\alpha}, B_i^{p\alpha}, D_i^{p\alpha}$ are obtained by extending lamination theory to the stiffened cross-section based on $\bar{\Phi}_i^*$ of each layer using Equation 3.24 and Equation 3.25. Determination of the thermal coefficients is analogous to the calculation for panel elastic stiffness presented in the previous section.

Thermal expansion vectors $\alpha_{A_i}^p, \alpha_{B_i}^p, \alpha_{D_i}^p$ are calculated from panel elastic stiffness matrices and panel thermal stiffness vectors:

$$\begin{aligned}
\{\alpha_A^p\} &= [A^p]^{-1} \{A^{p\alpha}\} \\
\{\alpha_B^p\} &= [B^p]^{-1} \{B^{p\alpha}\} \\
\{\alpha_D^p\} &= [D^p]^{-1} \{D^{p\alpha}\}
\end{aligned} \tag{3.26}$$

Equation 3.26 is taken from Equations 5.27, 5.28, and 5.29 in reference [2]. Thermal stress and moment resultants are calculated from Equations 5.22 and 5.23 of reference [2]:

$$\begin{Bmatrix} N^{thermal} \\ M^{thermal} \end{Bmatrix} = \begin{bmatrix} A^p & B^p \\ B^p & D^p \end{bmatrix} \begin{Bmatrix} \alpha_A^p \\ \alpha_B^p \end{Bmatrix} \Delta T - \begin{bmatrix} A^p & B^p \\ B^p & D^p \end{bmatrix} \begin{Bmatrix} \alpha_B^p \\ \alpha_D^p \end{Bmatrix} \Delta G \quad (3.27)$$

where ΔT is the difference between element reference plane temperature and global reference temperature and ΔG is the through-the-thickness temperature gradient. The NASTRAN and I-DEAS finite element programs use Equation 3.27 to compute thermal loads [6].

Residual thermal strains need to be added to the computed finite element strains in thermal analysis. This involves comparing free thermal growth of panel laminates to panel growth when forced to strain together as a unit [3].

3.4 Behavior unique to a panel construction type

Depending on the geometry of the stiffened panel cross-section, actual panel coefficients may deviate significantly from the basic formulation presented in Section 3.2. This thesis primarily investigated open-section stiffened panel coefficients. To determine the coefficients precisely, it is necessary to consider how the panels are joined between frames in a completed structure. This consideration has an effect on the panel shear and twisting coefficients $A_{33}^p, B_{33}^p, D_{33}^p$.

A panel stiffened with a longitudinal stringer has an increased ability to carry longitudinal membrane and bending loads. Also, for closed-cell stiffeners, additional stiffness is found in the in-plane transverse coefficients and panel shear and twisting coefficients.

3.5 Post-processing of stiffened panels

After a finite element model solution, shell stress resultants are obtained. As with laminates, panel stresses through-the-thickness are not linear but are discontinuous layer to layer. Using the Kirchoff hypothesis that plane sections remain plane and normal to the reference plane after deformation, reference plane strains and curvatures for the panel can be recovered through the relationship in Equation 3.13 rewritten as

$$\begin{Bmatrix} \varepsilon_i^o \\ \kappa_i \end{Bmatrix} = \begin{bmatrix} A_{ij} & B_{ij} \\ B_{ij} & D_{ij} \end{bmatrix}^{-1} \begin{Bmatrix} N_j \\ M_j \end{Bmatrix} \quad (3.28)$$

Strains at desired through-the-thickness locations of the panel can be determined from the linear relationship between reference plane strains, curvatures, and the distance from the reference plane

$$\varepsilon_i = \varepsilon_i^o + z\kappa_i \quad (3.29)$$

Given the properties of the corresponding laminate, the state of stress at a given location in panel can be obtained with

$$\sigma_i = \bar{Q}_{ij}\varepsilon_j \quad (3.30)$$

where \bar{Q}_{ij} is given by Equation 3.3.

For lamina failure tests, stresses may be transformed from the laminate coordinate system back to the fiber coordinate system for application of ply failure theories such as

those of Tsai-Wu and Tsai-Hill [5]. Strain-based instability formulae may be applied for stability analysis of the stiffened panel geometry. Detailed discussion of panel failure considerations is presented in reference [3].

4.0 DERIVATION OF PANEL COEFFICIENTS

The basic formulation of smeared panel coefficients for honeycomb sandwich, blade-stiffened, T-stiffened, and orthogrid panels are derived in this chapter. Stiffness terms are based on the design variables of the particular panel geometry. All coefficients are based on the surface outer mold line (OML) of the panel as the reference plane. Using an outer mold line formulation allows panel properties to shift into the vehicle so that finite element meshes remain constant and consistent as panel configurations are sized during an analysis. The shift is accounted for as unsymmetric property formulation. As panel design variables are changed, larger D_{ij}^p bending coefficient changes result but are balanced by corresponding changes in the B_{ij}^p membrane-bending coefficients.

4.1 Honeycomb sandwich panel

Although not having a stiffened panel configuration, a popular method of composite construction is the sandwich. Thin inner and outer layers of high strength material are separated by a thick low density core as shown in Figure 4.1. The outer sheets carry the membrane loads and the core transmits shear between the sheets in bending. The facesheets are often made of composite materials and a popular core material is "honeycomb", a material made of thin foils usually in the form of hexagonal cells [9].

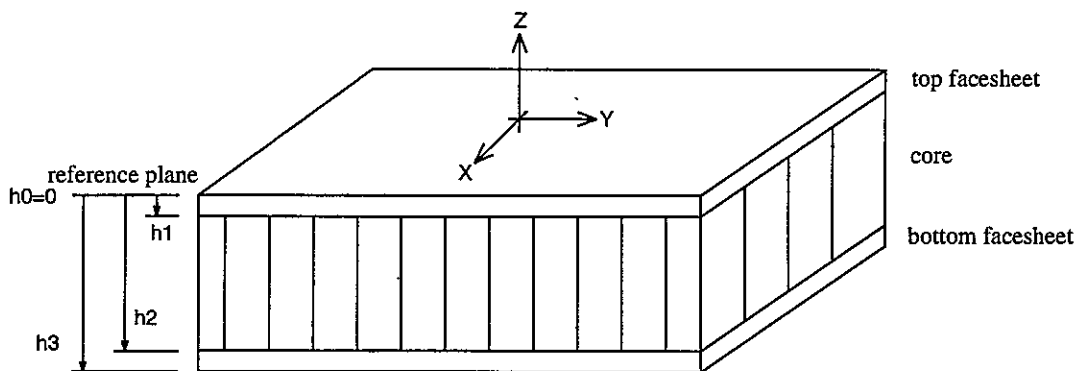


Figure 4.1: *Honeycomb sandwich panel.*

Stiffness properties of the honeycomb panel can be easily constructed from a direct application of classical lamination theory to the cross-section of the panel. Each facesheet contributes to all panel coefficients. The core is modeled as an orthotropic ply. Unlike a stringer stiffened panel where only longitudinal stiffness directly contributes, the honeycomb core behaves like an additional facesheet and contributes to all panel coefficients. Honeycomb panel coefficients are in the form:

$$\begin{aligned}
A_{ij}^p \Big|_{\text{honeycomb}} &= (\bar{Q}_{ij}^*)_{\text{top}} (h_0 - h_1) + (\bar{Q}_{ij}^*)_{\text{core}} (h_1 - h_2) + (\bar{Q}_{ij}^*)_{\text{bottom}} (h_2 - h_3) \\
2B_{ij}^p \Big|_{\text{honeycomb}} &= (\bar{Q}_{ij}^*)_{\text{top}} (h_0^2 - h_1^2) + (\bar{Q}_{ij}^*)_{\text{core}} (h_1^2 - h_2^2) + (\bar{Q}_{ij}^*)_{\text{bottom}} (h_2^2 - h_3^2) \\
3D_{ij}^p \Big|_{\text{honeycomb}} &= (\bar{Q}_{ij}^*)_{\text{top}} (h_0^3 - h_1^3) + (\bar{Q}_{ij}^*)_{\text{core}} (h_1^3 - h_2^3) + (\bar{Q}_{ij}^*)_{\text{bottom}} (h_2^3 - h_3^3)
\end{aligned} \tag{4.1}$$

Thermal panel vectors $A_i^\alpha, B_i^\alpha, D_i^\alpha$ are formulated similarly as:

$$\begin{aligned}
A_i^{p\alpha} \Big|_{\text{honeycomb}} &= (\bar{\Phi}_i^*)_{\text{top}} (h_0 - h_1) + (\bar{\Phi}_i^*)_{\text{core}} (h_1 - h_2) + (\bar{\Phi}_i^*)_{\text{bottom}} (h_2 - h_3) \\
2B_i^{p\alpha} \Big|_{\text{honeycomb}} &= (\bar{\Phi}_i^*)_{\text{top}} (h_0^2 - h_1^2) + (\bar{\Phi}_i^*)_{\text{core}} (h_1^2 - h_2^2) + (\bar{\Phi}_i^*)_{\text{bottom}} (h_2^2 - h_3^2) \\
3D_i^{p\alpha} \Big|_{\text{honeycomb}} &= (\bar{\Phi}_i^*)_{\text{top}} (h_0^3 - h_1^3) + (\bar{\Phi}_i^*)_{\text{core}} (h_1^3 - h_2^3) + (\bar{\Phi}_i^*)_{\text{bottom}} (h_2^3 - h_3^3)
\end{aligned} \tag{4.2}$$

It is important to remember that composite laminate properties are being applied to all panel coefficients derived in this chapter. The composite properties are represented in \bar{Q}_{ij}^* and $\bar{\Phi}_i^*$ as given by Equations 3.14, 3.15, and 3.25.

For the honeycomb panel, it is expected that the basic formulation presented in Equation 4.1 and Equation 4.2 will sufficiently and completely characterize the behavior. There are no stringers associated with the honeycomb sandwich and extension of lamination theory can be applied directly to the panel cross-section.

4.2 Blade-stiffened panel

The first example of a stiffened panel is a facesheet with reinforcing blades. It is a step toward increasing the ability of the panel to transmit longitudinal bending loads and increase compressive buckling stability.

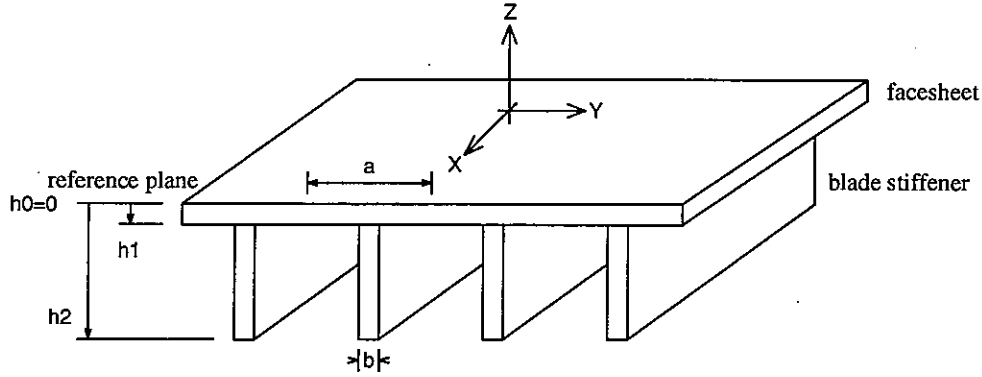


Figure 4.2: *Blade-stiffened panel.*

The facesheet forms the basis of the panel coefficients. The blades contribute only to the longitudinal coefficients A_{11}, B_{11}, D_{11} reflecting the average amount of blade material presented in the cross-section:

$$\begin{aligned}
 A_{11}^p|_{blade} &= (\overline{Q}_{11}^*)_{facesheet} (h_0 - h_1) + \left(\frac{b}{a}\right) (\overline{Q}_{11}^*)_{blade} (h_1 - h_2) \\
 2B_{11}^p|_{blade} &= (\overline{Q}_{11}^*)_{facesheet} (h_0^2 - h_1^2) + \left(\frac{b}{a}\right) (\overline{Q}_{11}^*)_{blade} (h_1^2 - h_2^2) \\
 3D_{11}^p|_{blade} &= (\overline{Q}_{11}^*)_{facesheet} (h_0^3 - h_1^3) + \left(\frac{b}{a}\right) (\overline{Q}_{11}^*)_{blade} (h_1^3 - h_2^3)
 \end{aligned} \tag{4.3}$$

Since the blades do not act as plates, as discussed in Section 3.2, the $(\overline{Q}_{11}^*)_{blade}$ term is obtained from the effective Young's modulus of the stringer laminate,

$$(\overline{Q}_{11})_{stringer} = \frac{1}{A_{11}^{-1}t} \quad (4.4)$$

where t is the laminate thickness.

All other panel coefficients are formulated from the facesheet alone:

$$\begin{aligned} A_{ij}^p|_{blade} &= (\overline{Q}_{ij})_{facesheet} (h_0 - h_1) \\ 2B_{ij}^p|_{blade} &= (\overline{Q}_{ij})_{facesheet} (h_0^2 - h_1^2) \\ 3D_{ij}^p|_{blade} &= (\overline{Q}_{ij})_{facesheet} (h_0^3 - h_1^3) \end{aligned} \quad (4.5)$$

Thermal panel vectors $A_i^\alpha, B_i^\alpha, D_i^\alpha$ follow similarly:

$$\begin{aligned} A_1^{p\alpha}|_{blade} &= (\overline{\Phi}_1^*)_{facesheet} (h_0 - h_1) + \left(\frac{b}{a}\right) (\overline{\Phi}_1^*)_{blade} (h_1 - h_2) \\ 2B_1^{p\alpha}|_{blade} &= (\overline{\Phi}_1^*)_{facesheet} (h_0^2 - h_1^2) + \left(\frac{b}{a}\right) (\overline{\Phi}_1^*)_{blade} (h_1^2 - h_2^2) \\ 3D_1^{p\alpha}|_{blade} &= (\overline{\Phi}_1^*)_{facesheet} (h_0^3 - h_1^3) + \left(\frac{b}{a}\right) (\overline{\Phi}_1^*)_{blade} (h_1^3 - h_2^3) \end{aligned} \quad (4.6)$$

For all other thermal coefficients:

$$\begin{aligned} A_i^{p\alpha}|_{blade} &= (\overline{\Phi}_i^*)_{facesheet} (h_0 - h_1) \\ 2B_i^{p\alpha}|_{blade} &= (\overline{\Phi}_i^*)_{facesheet} (h_0^2 - h_1^2) \\ 3D_i^{p\alpha}|_{blade} &= (\overline{\Phi}_i^*)_{facesheet} (h_0^3 - h_1^3) \end{aligned} \quad (4.7)$$

4.3 T-stiffened panel

A further step in increasing the efficiency of the panel for transmitting bending loads is adding a flange to the end of the blade resulting in a T-stiffened panel.

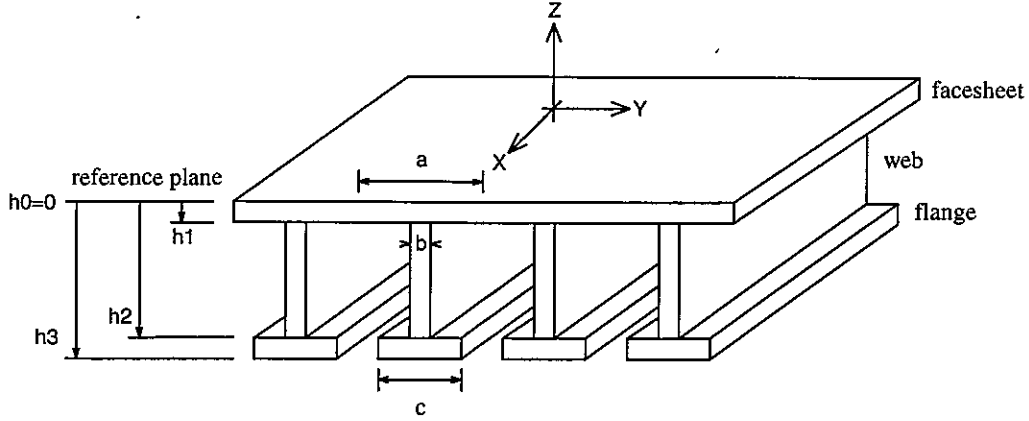


Figure 4.3: *T-stiffened panel.*

Because the longitudinal stringers contribute to the A_{11}, B_{11}, D_{11} terms, these are formulated as:

$$\begin{aligned}
 A_{11}^p|_T &= (\bar{Q}_{11}^*)_{facesheet} (h_0 - h_1) + \left(\frac{b}{a}\right) (\bar{Q}_{11}^*)_{web} (h_1 - h_2) + \left(\frac{c}{a}\right) (\bar{Q}_{11}^*)_{flange} (h_2 - h_3) \\
 2B_{11}^p|_T &= (\bar{Q}_{11}^*)_{facesheet} (h_0^2 - h_1^2) + \left(\frac{b}{a}\right) (\bar{Q}_{11}^*)_{web} (h_1^2 - h_2^2) + \left(\frac{c}{a}\right) (\bar{Q}_{11}^*)_{flange} (h_2^2 - h_3^2) \quad (4.8) \\
 3D_{11}^p|_T &= (\bar{Q}_{11}^*)_{facesheet} (h_0^3 - h_1^3) + \left(\frac{b}{a}\right) (\bar{Q}_{11}^*)_{web} (h_1^3 - h_2^3) + \left(\frac{c}{a}\right) (\bar{Q}_{11}^*)_{flange} (h_2^3 - h_3^3)
 \end{aligned}$$

As discussed, since the stringers do not act as plates, the $(\bar{Q}_{11}^*)_{web}$ and $(\bar{Q}_{11}^*)_{flange}$ terms are given by Equation 4.4.

In the basic formulation of panel coefficients, stiffness is obtained only in the direction of reinforcement from the stringers. Although it may appear that extra stiffness in the transverse direction is possible, it is not accounted for at this stage. Extra transverse stiffness as well as other stringer effects is investigated individually for each panel concept.

All other panel coefficients are formulated based on facesheet properties:

$$\begin{aligned}
A_{ij}^p|_T &= (\overline{Q}_{ij}^*)_{facesheet} (h_0 - h_1) \\
2B_{ij}^p|_T &= (\overline{Q}_{ij}^*)_{facesheet} (h_0^2 - h_1^2) \\
3D_{ij}^p|_T &= (\overline{Q}_{ij}^*)_{facesheet} (h_0^3 - h_1^3)
\end{aligned} \tag{4.9}$$

Thermal panel vectors $A_i^{p\alpha}, B_i^{p\alpha}, D_i^{p\alpha}$ follow similarly:

$$\begin{aligned}
A_1^{p\alpha}|_T &= (\overline{\Phi}_1^*)_{facesheet} (h_0 - h_1) + \left(\frac{b}{a}\right)(\overline{\Phi}_1^*)_{web} (h_1 - h_2) + \left(\frac{c}{a}\right)(\overline{\Phi}_1^*)_{flange} (h_2 - h_3) \\
2B_1^{p\alpha}|_T &= (\overline{\Phi}_1^*)_{facesheet} (h_0^2 - h_1^2) + \left(\frac{b}{a}\right)(\overline{\Phi}_1^*)_{web} (h_1^2 - h_2^2) + \left(\frac{c}{a}\right)(\overline{\Phi}_1^*)_{flange} (h_2^2 - h_3^2) \\
3D_1^{p\alpha}|_T &= (\overline{\Phi}_1^*)_{facesheet} (h_0^3 - h_1^3) + \left(\frac{b}{a}\right)(\overline{\Phi}_1^*)_{web} (h_1^3 - h_2^3) + \left(\frac{c}{a}\right)(\overline{\Phi}_1^*)_{flange} (h_2^3 - h_3^3)
\end{aligned} \tag{4.10}$$

For all other panel thermal coefficients:

$$\begin{aligned}
A_i^{p\alpha}|_T &= (\overline{\Phi}_i^*)_{facesheet} (h_0 - h_1) \\
2B_i^{p\alpha}|_T &= (\overline{\Phi}_i^*)_{facesheet} (h_0^2 - h_1^2) \\
3D_i^{p\alpha}|_T &= (\overline{\Phi}_i^*)_{facesheet} (h_0^3 - h_1^3)
\end{aligned} \tag{4.11}$$

4.4 Orthogrid panel

A blade-stiffened panel with stringers in both the longitudinal and transverse directions is known as an orthogrid panel. These panels have increased bending stiffness in both the longitudinal and transverse directions.

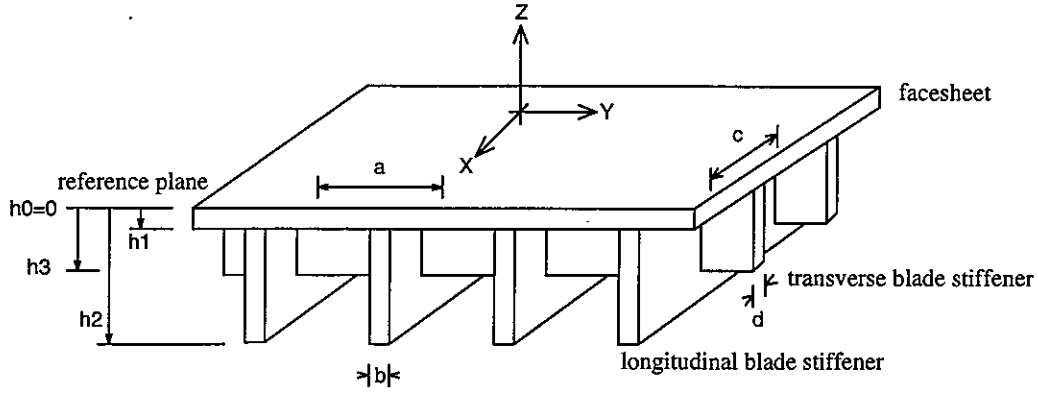


Figure 4.4: *Orthogrid panel.*

Because the blades contribute to the A_{11}, B_{11}, D_{11} and A_{22}, B_{22}, D_{22} terms, these coefficients are

$$\begin{aligned}
 A_{11}^p|_{orthogrid} &= (\bar{Q}_{11}^*)_{top} (h_0 - h_1) + \left(\frac{b}{a}\right) (\bar{Q}_{11}^*)_{blade1} (h_1 - h_2) \\
 2B_{11}^p|_{orthogrid} &= (\bar{Q}_{11}^*)_{top} (h_0^2 - h_1^2) + \left(\frac{b}{a}\right) (\bar{Q}_{11}^*)_{blade1} (h_1^2 - h_2^2) \\
 3D_{11}^p|_{orthogrid} &= (\bar{Q}_{11}^*)_{top} (h_0^3 - h_1^3) + \left(\frac{b}{a}\right) (\bar{Q}_{11}^*)_{blade1} (h_1^3 - h_2^3)
 \end{aligned} \tag{4.12}$$

$$\begin{aligned}
 A_{22}^p|_{orthogrid} &= (\bar{Q}_{22}^*)_{facesheet} (h_0 - h_1) + \left(\frac{d}{c}\right) (\bar{Q}_{11}^*)_{blade2} (h_1 - h_3) \\
 2B_{22}^p|_{orthogrid} &= (\bar{Q}_{22}^*)_{facesheet} (h_0^2 - h_1^2) + \left(\frac{d}{c}\right) (\bar{Q}_{11}^*)_{blade2} (h_1^2 - h_3^2) \\
 3D_{22}^p|_{orthogrid} &= (\bar{Q}_{22}^*)_{facesheet} (h_0^3 - h_1^3) + \left(\frac{d}{c}\right) (\bar{Q}_{11}^*)_{blade2} (h_1^3 - h_3^3)
 \end{aligned} \tag{4.13}$$

As discussed, since the stringers do not act as plates, the $(\bar{Q}_{11}^*)_{blade1}$ and $(\bar{Q}_{11}^*)_{blade2}$ terms are given by Equation 4.4.

For all other panel coefficients:

$$\begin{aligned}
A_{ij}^p \Big|_{orthogrid} &= (\overline{Q}_{ij}^*)_{facesheet} (h_0 - h_1) \\
2B_{ij}^p \Big|_{orthogrid} &= (\overline{Q}_{ij}^*)_{facesheet} (h_0^2 - h_1^2) \\
3D_{ij}^p \Big|_{orthogrid} &= (\overline{Q}_{ij}^*)_{facesheet} (h_0^3 - h_1^3)
\end{aligned} \tag{4.14}$$

Thermal panel vectors $A_i^\alpha, B_i^\alpha, D_i^\alpha$ follow:

$$\begin{aligned}
A_1^{p\alpha} \Big|_{orthogrid} &= (\overline{\Phi}_1^*)_{facesheet} (h_0 - h_1) + \left(\frac{b}{a}\right) (\overline{\Phi}_1^*)_{blade1} (h_1 - h_2) \\
2B_1^{p\alpha} \Big|_{orthogrid} &= (\overline{\Phi}_1^*)_{facesheet} (h_0^2 - h_1^2) + \left(\frac{b}{a}\right) (\overline{\Phi}_1^*)_{blade1} (h_1^2 - h_2^2) \\
3D_1^{p\alpha} \Big|_{orthogrid} &= (\overline{\Phi}_1^*)_{facesheet} (h_0^3 - h_1^3) + \left(\frac{b}{a}\right) (\overline{\Phi}_1^*)_{blade1} (h_1^3 - h_2^3)
\end{aligned} \tag{4.15}$$

$$\begin{aligned}
A_2^{p\alpha} \Big|_{orthogrid} &= (\overline{\Phi}_2^*)_{facesheet} (h_0 - h_1) + \left(\frac{d}{c}\right) (\overline{\Phi}_2^*)_{blade2} (h_1 - h_3) \\
2B_2^{p\alpha} \Big|_{orthogrid} &= (\overline{\Phi}_2^*)_{facesheet} (h_0^2 - h_1^2) + \left(\frac{d}{c}\right) (\overline{\Phi}_2^*)_{blade2} (h_1^2 - h_3^2) \\
3D_2^{p\alpha} \Big|_{orthogrid} &= (\overline{\Phi}_2^*)_{facesheet} (h_0^3 - h_1^3) + \left(\frac{d}{c}\right) (\overline{\Phi}_2^*)_{blade2} (h_1^3 - h_3^3)
\end{aligned} \tag{4.16}$$

$$\begin{aligned}
A_3^{p\alpha} \Big|_{orthogrid} &= (\overline{\Phi}_3^*)_{facesheet} (h_0 - h_1) \\
2B_3^{p\alpha} \Big|_{orthogrid} &= (\overline{\Phi}_3^*)_{facesheet} (h_0^2 - h_1^2) \\
3D_3^{p\alpha} \Big|_{orthogrid} &= (\overline{\Phi}_3^*)_{facesheet} (h_0^3 - h_1^3)
\end{aligned} \tag{4.17}$$

4.5 Notes on derived panel coefficients

In Sections 4.1 to 4.4, coefficients were derived for honeycomb, blade-stiffened, T-stiffened, and orthogrid panels. In general, these panel coefficients are formulated using composite laminate construction. In Chapter 5, panel coefficients obtained from 3-D finite element models are used for reference. It is expected that behavior unique to

each panel concept must be quantified to expand the derived coefficients to match the reference panel coefficients.

5.0 ANALYSIS AND DISCUSSION

This chapter presents comparisons of the panel coefficients formulated in Chapter 4 to reference panel coefficients obtained from 3-D shell finite element models. The assumption used in Equation 3.14 for simplification of the use of composite laminate properties is examined. Results of the finite element analysis are discussed and additional stiffness terms are explored in order to fully characterize panel coefficients derived in Chapter 4.

5.1 Method of obtaining reference panel coefficients

The validity of elastic smeared panel coefficients derived in Chapter 4 can be assessed by comparison with results from detailed 3-D shell finite element models. From consideration of the panel constitutive relationship:

$$\begin{Bmatrix} N_i \\ M_i \end{Bmatrix} = \begin{bmatrix} A_{ij}^p & B_{ij}^p \\ B_{ij}^p & D_{ij}^p \end{bmatrix} \begin{Bmatrix} \varepsilon_j^o \\ \kappa_j \end{Bmatrix} \quad (5.1)$$

unit strain and curvature boundary conditions can be defined for the 3-D panel models and reaction forces calculated during model solution will provide entries from the A^p , B^p , and D^p matrices. For example, a unit x-strain applied to a reference model will produce $A_{11}^p, A_{21}^p, B_{11}^p, B_{21}^p$ and a unit x-curvature will produce $B_{11}^p, B_{21}^p, D_{11}^p, D_{21}^p$. For convenience, rigid elements were applied such that the edges of the modeled panel enforced the unit applied loads and reaction forces were obtained at one node per edge. Dividing reaction forces by the length of the edge provides stiffness coefficients. For the stiffening concepts explored, the detailed 3-D finite element models were constructed and solved using the I-DEAS general purpose finite element software.

5.2 Use of effective reduced laminate stiffness

An important assumption for efficient formulation of panel coefficients was that the laminate A matrix sufficiently characterized composite material properties used in the stiffened panel cross-section. The use of effective isotropic properties reduces complexity in compiling panel coefficients from full ply information of each laminate comprising the panel. The errors introduced by this idealization were examined for impact on formulated panel coefficients. A laminate lay-up of $[0/+45/-45/90]_8$ with unidirectional graphite-epoxy lamina properties $E_{11}= 2.1 \times 10^7$ psi, $E_{22}= 2.0 \times 10^6$ psi, $\nu_{12}= 0.21$, $G_{12}= 0.8 \times 10^6$ psi, and thickness of 0.0054 inch was used as a reference.

Table 5.1 shows the errors introduced for a single 8 ply lay-up, 16 ply lay-up, and 24 ply lay-up. The first 3 columns of coefficients are obtained using classical lamination theory which considers the individual properties of the plies stacked in the laminate. The approximated properties in the last 3 columns are obtained from a single ply of the same laminate thickness with isotropic properties defined in Equation 3.14. No errors are expected in the approximated A_{ij}^* terms since these are the basis of the isotropic properties. However, significant error results in the approximated D_{ij}^* bending terms. Since the D_{ij}^* are functions of the distances from the reference plane cubed, the bending coefficients are in significant error for approximating thin lay-ups. Because of the symmetric balanced laminate used, membrane shear-extension coupling terms A_{13}, A_{23} are zero. However twisting-bending coupling terms D_{13}, D_{23} are generally non-zero and cannot be recovered since A_{13}, A_{23} used in Equation 3.14 are always zero in this case. Generally D_{13}, D_{23} are small compared to other bending coefficients and can be ignored. Laminates which have zero D_{13}, D_{23} terms are called specially orthotropic.

term	Classical Lamination Theory			Single ply with isotropic properties		
	8 plies	16 plies	24 plies	8 plies	16 plies	24 plies
A_{11}	3.960×10^5	7.920×10^5	1.188×10^6	3.960×10^5	7.920×10^5	1.188×10^6
A_{22}	3.960×10^5	7.920×10^5	1.188×10^6	3.960×10^5	7.920×10^5	1.188×10^6
A_{33}	1.375×10^5	2.749×10^5	4.124×10^5	1.375×10^5	2.749×10^5	4.124×10^5
A_{12}	1.211×10^5	2.422×10^5	3.633×10^5	1.211×10^5	2.422×10^5	3.633×10^5
D_{11}	1.006×10^2	5.798×10^2	1.780×10^3	6.159×10^1 (-38.8%)	4.927×10^2 (-13.7%)	1.663×10^3 (-6.6%)
D_{22}	2.853×10^2	4.266×10^2	1.564×10^3	6.159×10^1 (+115.8%)	4.927×10^2 (+15.5%)	1.663×10^3 (+6.3%)
D_{33}	1.838×10^1	1.650×10^2	5.682×10^2	2.138×10^1 (+16.3%)	1.710×10^2 (+3.6%)	5.772×10^2 (+1.6%)
D_{12}	1.584×10^1	1.447×10^2	4.995×10^2	1.884×10^1 (+19.0%)	1.507×10^2 (+4.2%)	5.085×10^2 (+1.8%)
D_{13}	6.009×10^0	1.202×10^1	1.803×10^1	0 (-100%)	0 (-100%)	0 (-100%)
D_{23}	6.009×10^0	1.202×10^1	1.803×10^1	0 (-100%)	0 (-100%)	0 (-100%)

Table 5.1: Comparison of approximated laminate properties to classical lamination theory using $[0/+45/-45/90]_n$ lay-up with 8, 16, and 24 plies.

As the number of plies and the thickness of the laminate increases, the approximated bending coefficients converge towards the full ply formulation values given by classical lamination theory. For example, longitudinal bending stiffness D_{11} is underestimated by 38.8% for 8 plies and by only 6.6% for 24 plies. Averaged laminate properties work very well if the magnitude of the approximated bending coefficient is

sufficiently large compared to the magnitude of the corresponding coefficient of a single lay-up of the approximated laminate.

It is concluded that using Equation 3.14 is an excellent way to characterize panel laminate information and avoid the complexity of full lamina information for sufficiently thick laminates. However, for approximating thin laminates, it is necessary to use the full D bending laminate information to achieve a high level of accuracy. For the panel coefficients derived in Chapter 4, the stiffened coefficients A_{11}, B_{11}, D_{11} which are many times larger than the bending stiffness of a single lay-up, will be very accurately formulated using isotropic properties. However, since all other panel coefficients are formulated based on the facesheet alone, it is necessary to use the D bending matrix of the facesheet laminate to model thin facesheets accurately.

5.3 Panel coefficient analysis

For the open-section stringer geometry explored in this work it was found that the basic formulation of panel coefficients agrees exactly with 3-D finite element modeling with a few exceptions. Unlike closed-section stringers where panel in-plane transverse bending stiffness was significantly affected, no corresponding additional stiffness is realized for open-section stringers. It was found that only the $A_{33}^p, B_{33}^p, D_{33}^p$ shear and twisting panel coefficients must be modified for an open-section stringer. The amount of additional stiffness depends on how the panel stringers are supported between panel frames.

The simplest case is for panels whose stringers are not anchored to frames. In panel shear, the A_{33}^p term does not deviate from the basic formulation where only shear stiffness of the facesheet is included. This is expected since the stringers are not effectively loaded when the facesheet is put into shear deformation. However, panel twisting reveals that significant changes must be made to the D_{33}^p term to fully characterize panel behavior. Additional twisting stiffness results from "strips" of material

in the open-section stringer resisting panel twisting which can be included by considering torsion of open-section beams. This result can be extended to any other open-section stiffening concept with free stringers not considered in this work such as a J-stiffened panel.

A complex situation arises for panels with stringers built-in to the frames between panels. Considering the stringer alone, additional stiffness results from stringer bending and its deformation is a cubic S shape. This behavior can easily be quantified when the stringer is not attached to the panel. However, when the facesheet interacts with the stringer, part of the stringer is forced to follow the linear deformation of the facesheet instead of the S shape. The resulting complex facesheet-stringer deformation is stiffer than what is realized in stringer bending alone and increases panel shear stiffness term A_{33}^p .

Because of the complicated interaction between facesheet and stringer, it is difficult to quantify the additional stiffness for the panel A_{33}^p coefficient. The amount of stiffness required is several percent of the A_{33}^p facesheet coefficient if the stringer has a flange and hence a large moment of inertia about the out-of-plane axis. For a blade stringer, the amount of stiffness was found to be insignificant.

Equally complex is the facesheet and stringer interaction in panel twisting. The solution for torsion of an open-section beam with built-in ends might be applied. However, the interaction between the stringer and the facesheet causes a linear deformation for part of the stringer. Additional torsion is needed to achieve the same rotational deformation. However, quantifying the amount of additional stiffness is difficult because of the complex boundary conditions.

Similar facesheet and stringer interaction behavior affects the orthogrid. Again, only the coefficients $A_{33}^p, B_{33}^p, D_{33}^p$ are affected. The stringers in both longitudinal and transverse directions act as closed cells which increase panel shear and twisting stiffness. Additional stiffness is obtained from the stringers acting in bending, although interaction

with the facesheet makes it difficult to quantify the extra stiffness. Additional panel torsion stiffness is realized that dominates D_{33}^p . Therefore the orthogrid coefficients defined in Section 4.4 underestimate $A_{33}^p, B_{33}^p, D_{33}^p$ significantly.

Since local geometry changes occur during the shear and torsional loading of a panel with stringers with built-in ends, panel behavior in other modes may be affected. Because of the complicated nature of this problem, completing the panel coefficients for these cases is beyond the scope of this work.

5.4 Additional stiffness for panels with unsupported stringers

For panels whose stringers are not built-in to frames, it was found that no additional consideration is needed beyond the basic panel coefficient formulation except for the twisting coefficient D_{33}^p . For the hat panel, the closed-cell construction dominated D_{33}^p over the twisting stiffness of the facesheet alone (which is the only stiffness accounted for in the basic formulation of panel coefficients outlined in Section 3.2). Even though open-section beams are weaker in torsion than closed-section beams, additional stiffness is needed to fully characterize the D_{33}^p twisting coefficient.

Considering an open-section beam in torsion, angle of twist is related to torque by

$$\theta = \frac{TL}{JG} \quad (5.2)$$

where T is the applied torque, L is the length of the beam, G is the shear modulus, and J is the torsion constant

$$J = \sum \frac{st^3}{3} \quad (5.3)$$

Here s is the base and t is the thickness of the flanges composing the open-section beam. Application of Equation 5.3 can be used to complete the D_{33}^p twisting coefficient for free open-section stringers:

$$D_{33}^p = \frac{1}{a} \sum_{i=1}^n s_i D_{33,i} \quad (5.4)$$

where s_i is the length of the strip, a is the spacing between stringers, and n is the number of sections. Use of Equation 5.4 is illustrated for a T-stiffened panel in Figure 5.1. For $n = 1$, $s_1 = a$ and the facesheet twisting stiffness of the basic formulation is obtained. The magnitude of the additional twisting stiffness contributed by the stringer is on the order of the facesheet twisting stiffness, but is small compared to dominating twisting stiffness resulting from closed-section stringers. This additional stiffness is independent of the reference plane of the panel. In addition, no significant additions to the shear-twisting coupling coefficient B_{33}^p were found.

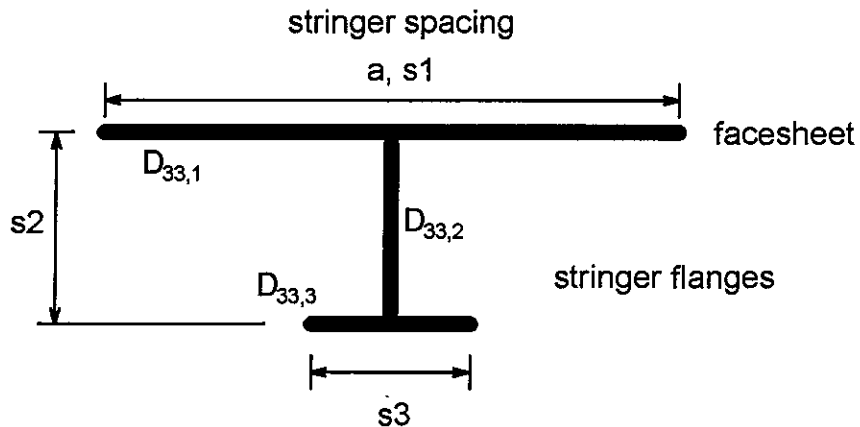


Figure 5.1: Open-section beam geometry for T-stiffened panel.

5.5 Summary of derived panel coefficients

The honeycomb sandwich coefficients derived in Chapter 4 are correct as formulated. For the blade-stiffened, T-stiffened, and for any panel with open-section

stringers which are free between frames, the basic formulation of coefficients are correct except for the D_{33}^p twisting coefficients which are replaced by Equation 5.4. The orthogrid panel coefficients are correct except for $A_{33}^p, B_{33}^p, D_{33}^p$ where closed cells formed by stringers significantly increase panel shear and twisting stiffness. For panels whose open-section stringers are built-in between frames, small increases are realized in A_{33}^p and dominating increases are exhibited in D_{33}^p . Complete determination of panel coefficients for the orthogrid and panels with built-in stringers has not been determined in this work.

Figure 5.2 defines applied loads and boundary conditions on the blade-stiffened and T-stiffened panels shown in Figures 5.3 and 5.4. Out-of-plane deflections predicted using 3-D finite element models are compared to those from 2-D elements using derived panel coefficients. Panel displacement in the normal direction is plotted. Differences between the 3-D model and the planar mesh are on the order of 1% for these two examples.

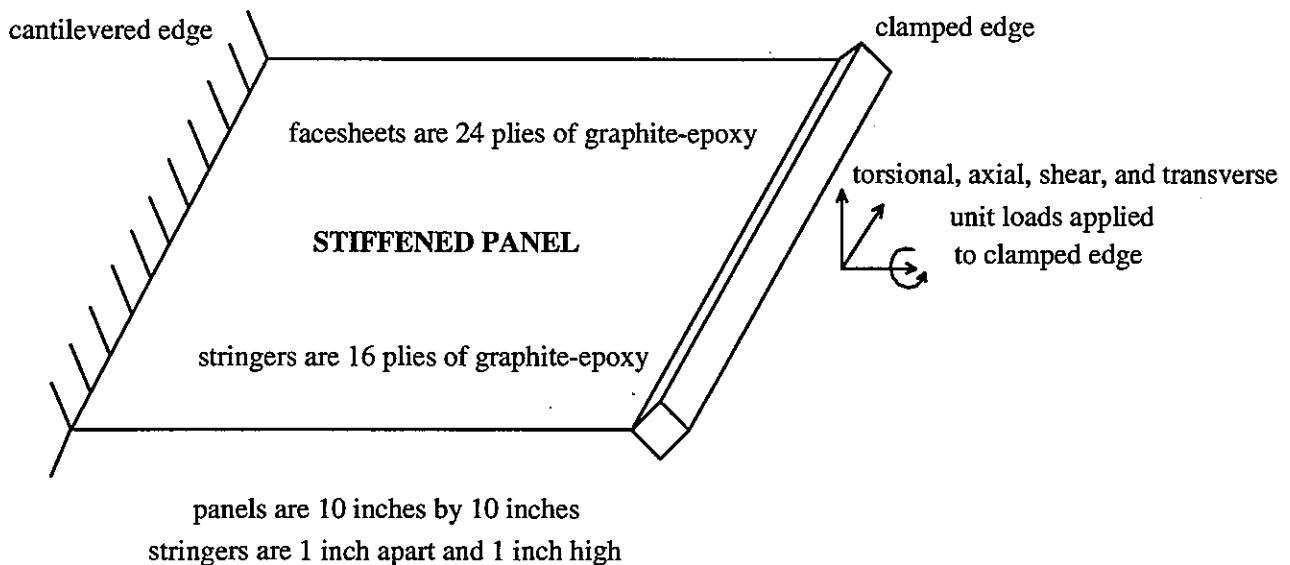
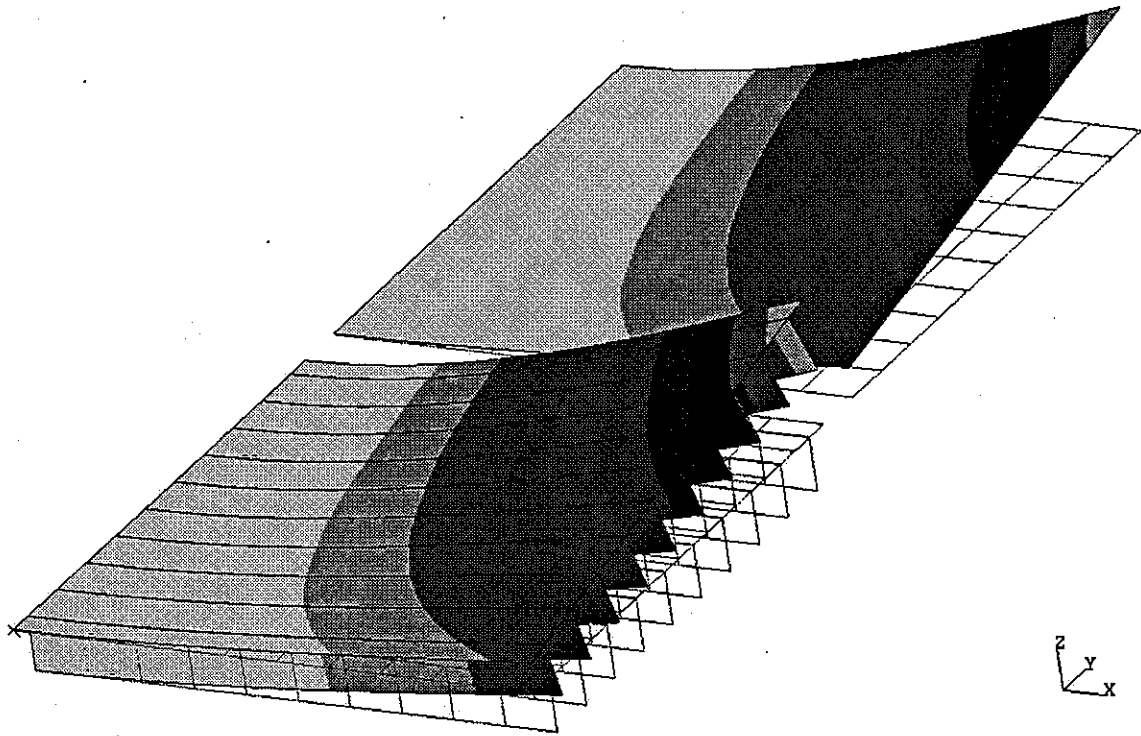
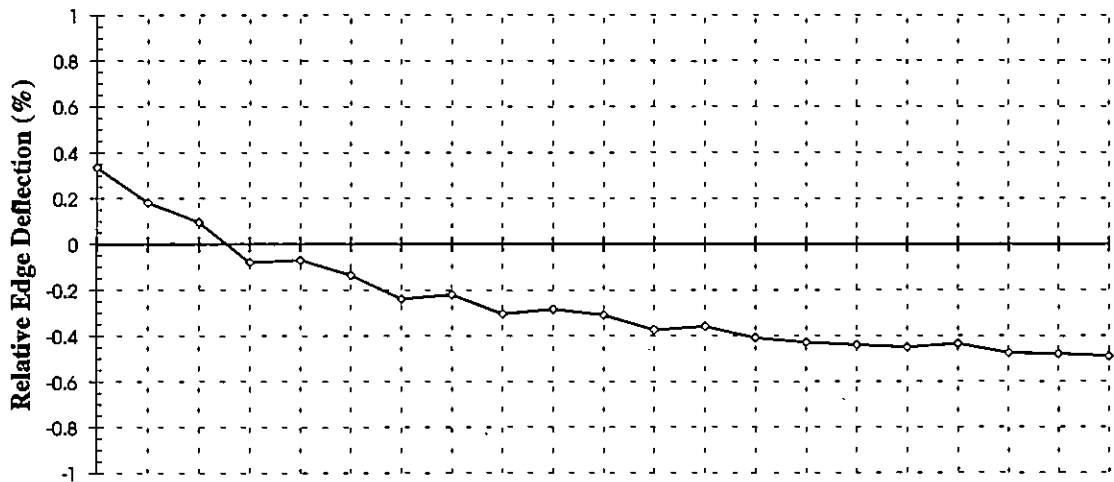


Figure 5.2: *Boundary conditions and applied loads for stiffened panel examples.*

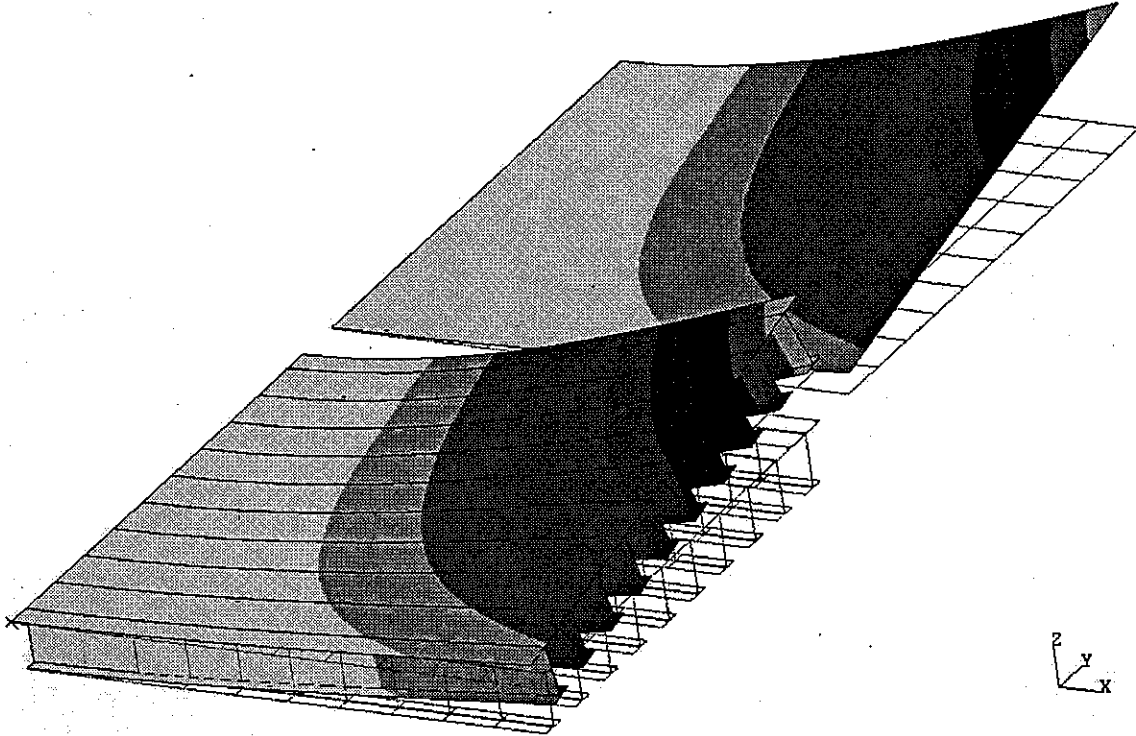


Relative Edge Deflection for Blade-Stiffened Panel

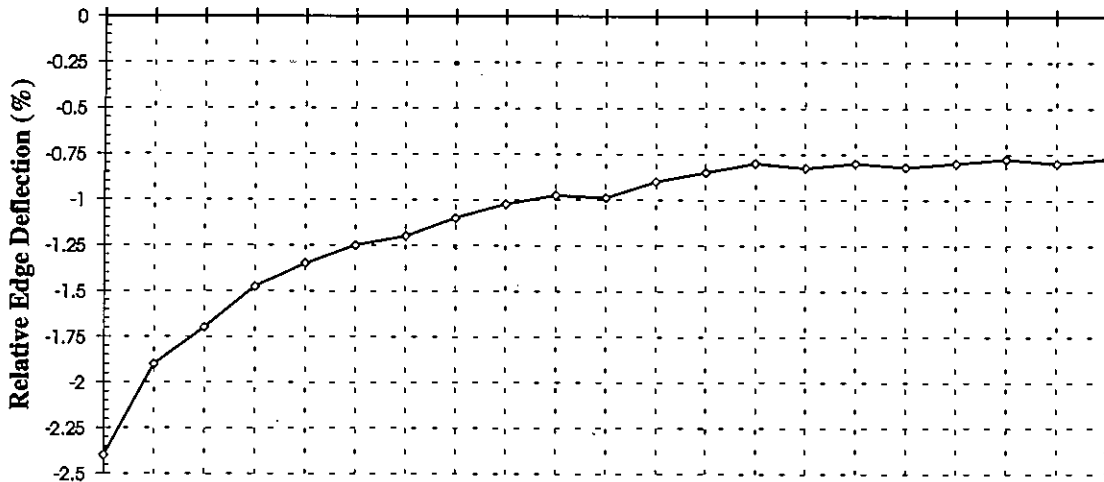


Location along front edge towards maximum out-of-plane deflection

Figure 5.3: *Displacement in the out-of-plane direction (top) and percent difference of edge deflection (bottom) for blade-stiffened composite panel.*



Relative Edge Deflection for T-Stiffened Panel



Location along front edge towards maximum out-of-plane deflection

Figure 5.4: Displacement in the out-of-plane direction (top) and percent difference of edge deflection (bottom) for T-stiffened composite panel.

6.0 CONCLUDING REMARKS

Equivalent elastic coefficients for honeycomb, blade-stiffened, T-stiffened, and orthogrid composite panels were derived using a method developed under NASP research. These coefficients were compared to reference coefficients obtained by analyzing 3-D shell finite element models. Coefficients for the honeycomb sandwich panel were obtained from direct application of the method. Unlike the closed-section hat-stiffened panel previously studied, the open-section stiffened panels explored in this work were fully characterized by the basic formulation of panel coefficients except for panel shear and twisting. The basis of completing these coefficients depends on stringer geometry and how the stringers are attached between frames. For panels with free stringers, open-section stringer geometry contributes torsional stiffness that was quantified to complete the panel twisting coefficients.

A more complicated situation was found for panels with built-in stringers. In panel shear, 3-D finite element analysis results show greater panel stiffness when compared to the basic formulation which considers facesheet stiffness only. Panel twisting stiffness is dominated by this effect. A complicated interaction between the facesheet and stringers occurs making it difficult to accurately predict the additional stiffness for these coefficients. Local geometry changes occurring from shear and torsion loading of the panel may cause deviations in other panel coefficients. Similar effects occur for the orthogrid panel. Analysis of the complex behavior for these cases is beyond the scope of this thesis.

With the precise panel coefficients determined, solution and post-processing of finite element models using this method can be performed accurately and efficiently. Finite element solution provides stress resultants which can be used to obtain strain at desired locations in the panel. Stability analysis is sensitive to the elastic panel coefficients and it is necessary to obtain accurate coefficients for post-processing of the panel. Since the

panel thermal coefficients are functions of the elastic coefficients, precise formulation of the elastic coefficients is necessary for accurate modeling of panel thermal behavior.

For the open-section panels considered, the most significant future work would be to quantify the complex interaction between the facesheet and stringer for built-in stringers which affects the panel shear and twisting coefficients. The extent of this interaction is a function of the relative bending stiffness of the facesheet and of the stringers. For the orthogrid panel, these coefficients are affected by the closed-sections formed by stringers. The smeared panel coefficient method can be extended to other stiffened panel concepts such as the isogrid where a similar stringer and facesheet interaction is expected.

It is concluded from this research that the smeared panel coefficient method is an excellent way to accurately model composite stiffened panels using single finite elements. Accurate and efficient vehicle analysis can be performed with only a coarse mesh of planar finite elements. A vehicle sizing code that varies panel dimensions based on post-processing failure and stability analyses of finite element solutions can be implemented with this method for accurate vehicle structural analysis and weight estimation. The ST-SIZE sizing code developed under NASP research uses this method to model hat-stiffened panels. The single panel type in the ST-SIZE code using smeared panel coefficients has been augmented with honeycomb sandwich and open-section composite panel formulation outlined in this work.

7.0 REFERENCES

- [1] Collier, C.S., "A General Method for Structural Analysis and Sizing of Composite Stiffened Panels Using 2-D Finite Element Models," Proceedings of the National Aero-Space Plane Mid-Term Technology Review, Monterey, CA, April 21-24, 1992, paper No. 212.
- [2] Collier, C.S., *Composite Stiffened Panels: Part I - Stiffness, Thermal Expansion, and Thermal Bending Formulation for Finite Element Analysis*, April 1992, NASP CR 1134.
- [3] Collier, C.S., "Thermoelastic Analysis of Aero-Space Planes," Proceedings of the National Aero-Space Plane Technology Review, Monterey, CA, April 13-16, 1993, paper No. 100.
- [4] Collier, C.S., "Thermoelastic Formulation of Stiffened, Unsymmetric Composite Panels for Finite Element Analysis of High Speed Aircraft," AIAA/ASME/ASCE/AHS/ASC 35th Structures, Dynamics, and Materials Conference, Hilton Head, SC, April 18-20, 1994, Paper No. AIAA-94-1579.
- [5] Halpin, J.C., *Primer on Composite Materials: Analysis*, Technomic Publishing Corporation, Lancaster, PA, 1984.
- [6] I-DEAS Master Series On-line Help, "Understanding Laminate Material Properties," Structural Dynamics Research Corporation, 1994.
- [7] Jones, R.M., *Mechanics of Composite Materials*, Hemisphere Publishing Corporation, Washington, DC, 1975.
- [8] Megson, T.H.G, *Aircraft Structures for Engineering Students*, Halsted Press, New York, NY, 1990.
- [9] Peery, D.J., Azar, J.J., *Aircraft Structures*, McGraw-Hill Inc., 1982.
- [10] Whitney, J.M., *Structural Analysis of Laminate Anisotropic Plates*, Technomic Publishing Corporation, Lancaster, PA, 1987.

